



**Calhoun: The NPS Institutional Archive**

---

Theses and Dissertations

Thesis Collection

---

1985

Particle sizing in a solid rocket motor using the  
measurement of scattered light.

Kertadidjaja, Abubakar.

Monterey, California. Naval Postgraduate School

---

<http://hdl.handle.net/10945/21483>



Calhoun is a project of the Dudley Knox Library at NPS, furthering the precepts and goals of open government and government transparency. All information contained herein has been approved for release by the NPS Public Affairs Officer.

**Dudley Knox Library / Naval Postgraduate School**  
**411 Dyer Road / 1 University Circle**  
**Monterey, California USA 93943**

<http://www.nps.edu/library>



DODGE K. K. LIBRARY  
NAVAL POSTGRADUATE SCHOOL  
MONTEREY, CALIFORNIA 93943





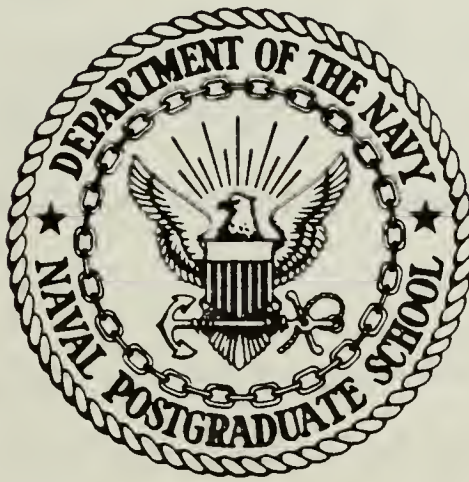






# NAVAL POSTGRADUATE SCHOOL

Monterey, California



## THESIS

PARTICLE SIZING IN A SOLID ROCKET MOTOR  
USING THE MEASUREMENT OF SCATTERED LIGHT

by

Kertadidjaja Abubakar

March 1985

Thesis Advisor:

D. W. Netzer

Approved for public release; distribution unlimited

T221559





REPORT DOCUMENTATION PAGE		READ INSTRUCTIONS BEFORE COMPLETING FORM
1. REPORT NUMBER	2. GOVT ACCESSION NO.	3. RECIPIENT'S CATALOG NUMBER
4. TITLE (and Subtitle) Particle Sizing in a Solid Rocket Motor Using the Measurement of Scattered Light		5. TYPE OF REPORT & PERIOD COVERED Master's thesis; March 1985
		6. PERFORMING ORG. REPORT NUMBER
7. AUTHOR(s) Kertadidjaja Abubakar		8. CONTRACT OR GRANT NUMBER(s)
9. PERFORMING ORGANIZATION NAME AND ADDRESS Naval Postgraduate School Monterey, California 93943		10. PROGRAM ELEMENT, PROJECT, TASK AREA & WORK UNIT NUMBERS F04611-84-x-0009
11. CONTROLLING OFFICE NAME AND ADDRESS Air Force Rocket Propulsion Laboratory Edwards, California 93523		12. REPORT DATE March 1985
		13. NUMBER OF PAGES 62
14. MONITORING AGENCY NAME & ADDRESS (if different from Controlling Office)		15. SECURITY CLASS. (of this report)
		15a. DECLASSIFICATION/ DOWNGRADING SCHEDULE
16. DISTRIBUTION STATEMENT (of this Report) Approved for public release; distribution unlimited		
17. DISTRIBUTION STATEMENT (of the abstract entered in Block 20, if different from Report)		
18. SUPPLEMENTARY NOTES		
19. KEY WORDS (Continue on reverse side if necessary and identify by block number) Diffractively scattered light Solid propellant Particle sizing		
20. ABSTRACT (Continue on reverse side if necessary and identify by block number) An experimental investigation was conducted to determine the feasibility of measuring the change in particle size across the exhaust nozzle of a small solid propellant rocket motor. Light scattering measurements were made at small forward angles at the entrance and exit of the exhaust nozzle. The experimental technique was found to be practical, especially if used in conjunction with measurements of transmitted light of multiple wave lengths.		

Block 20 Contd.

However, the determination of  $D_{32}$  is difficult in the motor environment and is biased toward the larger particle in the size distribution. Particle size measurements were in reasonable agreement with sizes determined from collected exhaust products. Recommendations for further improvement of the apparatus are made.

Approved for public release; distribution is unlimited.

Particle Sizing in a Solid Rocket Motor  
Using the Measurement of Scattered Light

by

Kertadidjaja Abubakar  
Major, Indonesian Air Force  
B.S., Indonesian Air Force Academy, 1968

Submitted in partial fulfillment of the  
requirements for the degree of

MASTER OF SCIENCE IN AERONAUTICAL ENGINEERING

from the

NAVAL POSTGRADUATE SCHOOL  
March 1985

772813  
- 31902  
C. 2  
DUBLEY  
NAVAL  
MONTEREY: CALIFORNIA 0 1943

## ABSTRACT

An experimental investigation was conducted to determine the feasibility of measuring the change in particle size across the exhaust nozzle of a small solid propellant rocket motor. Light scattering measurements were made at small forward angles at the entrance and exit of the exhaust nozzle. The experimental technique was found to be practical, especially if used in conjunction with measurements of transmitted light of multiple wave lengths. However, the determination of  $D_{32}$  is difficult in the motor environment and is biased toward the larger particles in the size distribution. Particle size measurements were in reasonable agreement with sizes determined from collected exhaust products. Recommendations for further improvement of the apparatus are made.

# TABLE OF CONTENTS

I.	INTRODUCTION . . . . .	10
II.	BACKGROUND THEORY . . . . .	14
III.	EXPERIMENTAL APPARATUS . . . . .	16
	A. ROCKET MOTOR . . . . .	16
	B. LIGHT SCATTERING APPARATUS . . . . .	17
	C. DATA ACQUISITION SYSTEM AND DATA REDUCTION . .	17
IV.	RESULT AND DISCUSSION . . . . .	26
	A. INTRODUCTION . . . . .	26
	B. EXPERIMENTS USING THE SHORT MOTOR CAVITY LENGTH . . . . .	26
	C. SYSTEM CALIBRATION . . . . .	27
	D. NOZZLE EXHAUST MEASUREMENTS . . . . .	29
	E. NOZZLE ENTRANCE MEASUREMENTS . . . . .	30
V.	CONCLUSIONS AND RECOMMENDATIONS . . . . .	59
	LIST OF REFERENCES . . . . .	60
	INITIAL DISTRIBUTION LIST . . . . .	62

## LIST OF TABLES

I	Exhaust Nozzle Specification . . . . .	19
II	Light Source Specification . . . . .	25
III	Experimental Results from Short Motor . . . . .	32
IV	Experimental Results from Long Motor . . . . .	35



## LIST OF FIGURES

3.1	Modified Motor Component . . . . .	20
3.2	Installation of the Small Rocket Motor . . . . .	21
3.3	Schematic of the Short Motor . . . . .	22
3.4	Photograph of Light Scattering Apparatus Set-up . .	23
3.5	Schematic Diagram of Light Scattering Apparatus . .	24
4.1	D <sub>32</sub> Results by Curve Fit Method . . . . .	33
4.2	SEM Evaluation, 4.8% Al Propellant Short Motor . .	34
4.3	Curve Fit Method Using 82% Transmitted Light . . .	36
4.4	Curve Fit Method Using 55% Transmitted Light . . .	37
4.5	Curve Fit Method Using 29% Transmitted Light . . .	38
4.6	Two Angle Method Using 82% Transmitted Light . . .	39
4.7	Two Angle Method, 55% Transmitted Light . . . . .	40
4.8	Two Angle Method Using 29% Transmitted Light . . .	41
4.9	Non-metalized Propellant, 55% Attenuation . . . . .	42
4.10	$I(\theta)$ vs Theta ( $\theta$ ), Non-Metalized Propellant . . . .	43
4.11	Voltage vs Diode, Non-Metalized Propellant . . . . .	44
4.12	Voltage vs Diode, 4.8% Aluminum Propellant . . . . .	45
4.13	$I(\theta)$ vs Theta ( $\theta$ ), 4.8% Aluminum Propellant . . . .	46
4.14	Two-Angle Method, 4.8% Aluminum Propellant, Exhaust . . . . .	47
4.15	Collected Exhaust Particle, 4.8% Aluminum Propellant . . . . .	48
4.16	Curve Fit Method, 2% Aluminum Propellant, Exhaust . . . . .	49
4.17	Two-Angle Method, 2% Aluminum Propellant, Exhaust . . . . .	50
4.18	SEM Evaluation, 2% Aluminum Propellant, Exhaust . .	51
4.19	Voltage vs Diode, 0% Aluminum, Motor Cavity . . . .	52

4.20	I( $\theta$ ) vs Theta ( $\theta$ ), 0% Aluminum, Motor Cavity . . .	53
4.21	Voltage vs Diode, 4.8% Aluminum, Motor Cavity . . .	54
4.22	SEM Evaluation, 4.8% Aluminum, Motor Cavity . . .	55
4.23	I( $\theta$ ) vs Theta ( $\theta$ ), 2% Aluminum, Motor, Curve fit . . . . .	56
4.24	Two-Angle Method, 2% Aluminum, Motor Cavity . . .	57
4.25	SEM Evaluation, 2% Aluminum Propellant, Motor Cavity . . . . .	58

## ACKNOWLEDGEMENTS

I would like to acknowledge the contributions of individuals and organization of the Departement of Aeronautics, who have assisted in this Thesis project.

Innumerable thanks to Professor David W. Netzer for his advice and assistance, making it a pleasure to study in the Combustion Laboratory.

Finally, I am grateful to my wife and children for their patience, understanding, and encouragement.

## I. INTRODUCTION

Aluminum is added to solid propellants to increase performance and to suppress high-frequency combustion instability. Although the measured specific impulse of such propellants is higher than that of the base propellant without aluminum, the specific impulse efficiency of the aluminized propellant is lower. The lower efficiency is largely due to the presence of condensed aluminum oxide in the exhaust. However, there are instances where incomplete combustion of the metal may be a major source of performance loss. A small amount of a variety of additives in addition to aluminum (aluminum oxide, zirconium, etc) are used in reduced-smoke propellants for acoustic stabilization. The metallic additives generally burn in the gas phase after leaving the propellant surface, resulting in small (less than 2 micron) condensed particles. The completeness of this mode of combustion has a significant influence on the combustion efficiency [Refs. 1,2]. Some particles leave the surface immediately and others agglomerate on the surface before leaving. Particle burn-out is often accompanied by break-up of a metallic oxide cap. This results in larger (5 to 15 micron) particles. The oxide particle distribution is then, often bimodal. The larger particles are more important in the determination of two-phase flow losses in the exhaust nozzle since they are the ones which, in principle, could be affected through propellant changes. The metal and metal oxide particles result in chemical and physical losses which are not present in non-metalized propellant combustion. The solid particles and or liquid droplets are not in equilibrium with the gaseous combustion products. They are also not uniform in size and can change size as they traverse

through the propellant grain port and the nozzle. There are several rather complex analytical programs [Ref. 3] which model the important processes of momentum and thermal energy exchange between the solid, liquid, and gaseous phases as well as particle collisions, break-up, and wall collisions. However, these models remain semi-empirical and are generally based upon particle size distributions which were obtained from collected nozzle exhaust flows. Particle histories from the surface of the propellant to the nozzle exit remain largely unknown, due to the difficulty of making direct observations. Prediction of performance losses due to the presence of original metal and its oxides ( $\text{Al}_2\text{O}_3$ ) are very sensitive to the aluminium oxide particle size distribution, and no direct experimental data are available as a function of the position along the nozzle.

Two general methods have been used to incorporate two phase flow losses into motor efficiency predictions. The first correlates experimental particle size data with motor and propellant variables, as in the original Solid Propellant Performance Prediction Code (SPP) effort [Refs. 3,4,5]. The second approach calculates the exhaust particle size based on a critical Weber number [Ref. 5]. The improved SPP also uses an empirical approach [Ref. 5]. The two phase flow losses are strongly dependent upon the particle size data obtained experimentally. The final particle size is influenced by many factors, such as original powder size, operating environment (pressure, temperature, residence time, etc), motor configuration and throat size [Ref. 5].

Collecting exhaust products is feasible only for small rocket motors. Even then the techniques employed result in considerable variation in the measured size [Ref. 5]. Dobbins [Ref. 6] and Dobbins and Strand [Ref. 7] attempted to use an optical technique for measuring exhaust particle size and to compare the measurements with tank collected



exhaust results. The optical technique used was a three wave length transmission measurement. This technique requires knowledge of particle index of refraction and the standard deviation of the particle size distribution. The tank collection results were that exhaust particle size was not influenced significantly by either the propellant weight fraction of metal or the chamber pressure. The optical measurements generally yielded sizes which were too small and the results were inconsistent with the collected exhaust data. It was speculated that this discrepancy resulted from a bi-modal exhaust particle distribution.

Light transmission measurements have the advantage of being applicable to dense concentrations where multiple scattering occurs [Ref. 8]. However, the method works best for very small particles (on the order of the wave-length of the illumination source) and requires a-priori knowledge of the particle characteristics.

Light scattering measurements can also be used to determine particle size. It is an especially good technique when the particles are large compared to the wave length of the illuminating source [Ref. 9 to Ref. 18]. Ratioing intensities obtained at two forward scattering angles can be used to further reduce the complexity of the method. However, these techniques are generally considered to be applicable to systems where the transmittance is greater than approximately 90% in order to satisfy single scattering requirements.

A combination of light transmission and light scattering measurements [Ref. 16] appears to be well-suited for the solid rocket motor exhaust flow. However, experimental efforts are first needed to determine under what conditions (metal loadings, operating pressure, propellant ingredients, etc) light scattering measurements can be effectively made in this difficult environment.

At the Naval Postgraduate School an investigation was initiated to examine the applicability of the light scattering measurements to the solid rocket motor exhaust products [Ref. 19]. It was also decided to attempt to use the method both at the entrance and exhaust of the nozzle in order to determine if changes in particle size across the nozzle could be measured [Ref. 20]. After the initial efforts showed promise, the experimental apparatus and data acquisition/reduction processes were improved [Ref. 21]. In the latest effort the apparatus was calibrated using various sizes of glass, polystyrene, and aluminium oxide particles from 5 to 60 microns in diameter.

The purpose of this investigation was to use the apparatus developed in earlier efforts [Refs. 20,21] in an attempt to make particle size measurements across the exhaust nozzle of a small solid propellant rocket motor. Propellants with no aluminum and with small (2 - 4.8%) amounts of aluminum were to be used to determine the feasibility of the technique.



## II. BACKGROUND THEORY

The formulation of the theory for the scattering properties in the more general case of particles of arbitrary size and refractive index occurring in a polydispersion of finite optical depth is discussed in Reference 18. Mugele and Evans [Ref. 12] proposed using the Upper Limit Distribution Function (ULDF). Roberts and Webb [Ref. 11] concluded that the volume-surface mean diameter (Sauter)  $D_{32}$  of the polydispersion may be determined from the intensity of diffractively scattered light from spherical particles. This could be done with a good degree of accuracy without any knowledge of the general distribution type. Scattered light from large particles is dominated by Fraunhofer diffraction. Buchele [Ref. 17] has recently summarized the experimental technique for determining particle size by measuring diffractively scattered light. He has presented an expression for the light scattered of an angle ( $I(\theta)$ ) which closely matches the results of references 10 and 11.

$$I(\theta) = \text{EXP} - [.57\alpha\theta]^2$$

where

$$\alpha = \pi D / \lambda; D = \text{particle dia.}; \lambda = \text{wave length of light}$$

This function from Buchele, and the curve from Dobbins et al [Ref. 10] were used in the present study to evaluate the apparatus to be used with solid propellant rocket motors.

Two phase flow losses are often calculated in terms of  $D_{43}$ . In the SPP model [Ref. 5], an empirical formula is presented

$$D_{43} = 3.6304 D_f^{0.2932} (1 - e^{0.0008163 \xi_c P_c T})$$

where

$D_{43}$  = mass-weighted average diameter, micron

$D_f$  = nozzle diameter

$\xi_c$  =  $Al_2O_3$  concentration in chamber, g-mol/100 g

$P_c$  = chamber pressure

$T$  = average residence

Unfortunately, there is not a general method to a-priori relate the  $D_{32}$  obtained from scattering measurements to  $D_{43}$ .

### III. EXPERIMENTAL APPARATUS

#### A. ROCKET MOTOR

Two rocket motors were used in this investigation, referred to as the "short motor", and the "long motor". The short motor was the same as used by Cramer and Hansen [Ref. 20]. The long motor used the short motor, but was modified by increasing its length down-stream of the propellant grain by eight inches. Three types of exhaust nozzles were used in this experiment, one copper nozzle and two graphite nozzles. Specification are given in Table I. The reasons for the modifications are discussed below. A photograph of the motor components is presented in Figure 3.1. The installed motor is shown in Figure 3.2, and a schematic is shown in Figure 3.3. The nitrogen purge windows in the motor were always located at the entrance to the exhaust nozzle. The propellant grain was two inches in diameter and one inch in length with a web thickness of .725 inches. To obtain a period of steady state pressure in which to take data a cylindrically perforated grain design was used. Burning was also allowed on the aft end. A  $\text{BKNO}_3$  igniter was used, and was installed at the head of the motor. 12 VDC was used to heat a resistance wire to fire the igniter.

A sample of exhaust product was obtained by directing the exhaust into a partially end-capped, eight inch diameter, stainless steel tube. The products deposited on the walls and end plate were collected, repetitively cleaned and mounted for observation with a scanning electron microscope.

## B. LIGHT SCATTERING APPARATUS

A photograph of the apparatus is presented in Figure 3.4, and a schematic in Figure 3.5. The light sources consisted of an 8-milliwatt, Helium-Neon laser for the nozzle exhaust and an 5-milliwatt Argon laser for the nozzle entrance. The specifications for this equipment are given in Table II. The lasers were mounted on two parallel benches, one for the beam passing through the exhaust, and the other for the beam passing through the motor cavity at the exhaust nozzle entrance area. A beam expander/collimator was used with the Helium-Neon laser. Each beam was intercepted by a physical stop, located at approximately 30.5 centimeters from the motor center line. Each beam then passed through a narrow pass filter and condensing lens (focal length 50 centimeter). The scattered light was focused onto a linear diode array. The purpose of the filter was to prevent extraneous light from reaching the diodes. The photodiode arrays contained 1024 silicon photodiodes with 25 micron spacing.

## C. DATA ACQUISITION SYSTEM AND DATA REDUCTION

Details of the data acquisition system are presented in reference 21. The system controller was an HP 9836S computer. An HP 6942A multiprogrammer was used for rapid A/D conversion and storage. Two parallel channels were used. Four diode scans were made of the motor cavity beam and eight scans were made of the exhaust beam. Multiple scans were made to provide a more statistically valid measurement of particle size.

In the data reduction there were two methods for determining particle diameter. First, iterative graphics could be used to fit the theoretical profile (for specified  $D_{32}$  and scattered light intensity at zero degrees) to the experimentally obtained profile.



From this interactive procedure, a normalized intensity vs scattering angle profile was obtained. A "best-fit" yielded the mean particle diameter,  $D_{32}$ . The second method used the ratio of forward scattered light at two angles [Ref. 17]. The approximate equation for the polydispersion curve is [Ref. 17]

$$I(\theta) = \text{EXP} - \left[ .57 \alpha \theta \right]^2$$

This equation could be applied between any two diodes of the array. This gave

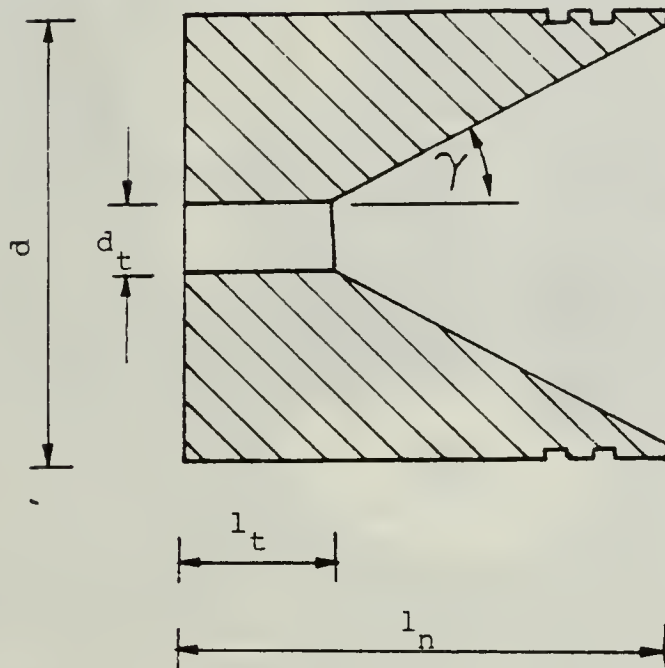
$$\frac{I_2}{I_1} = \text{EXP} - \left[ (\theta_2^2 - \theta_1^2) (.57 \pi / \lambda) \right]^2$$

Solving for the diameter gave :

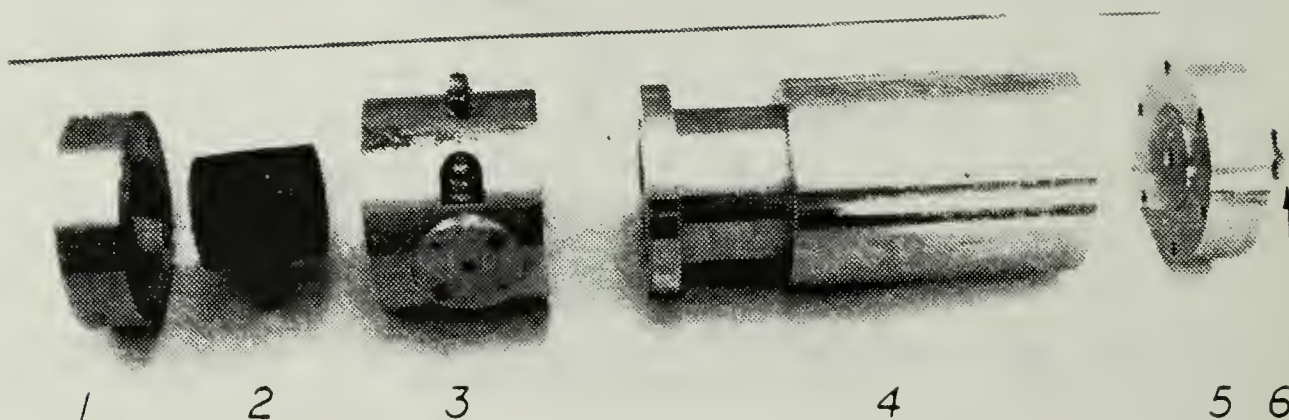
$$D_{32} = \left[ -\ln \left( \frac{I_2}{I_1} \right) (\lambda / .57 \pi)^2 / (\theta_2^2 - \theta_1^2) \right]^2$$

Various  $\theta_2/\theta_1$  ratios could be selected, as well as the starting angle. These results were presented graphically as particle size vs scattering angle for each angle ratio ( $\theta_2/\theta_1$ ). The data acquisition system also controlled when the data were taken during the motor firing. This was accomplished by monitoring a chamber pressure transducer and specifying a desired delay time after steady-state operation was achieved.

TABLE I  
Exhaust Nozzle Specification



Description	Copper Nozzle	Graphite Nozzle	Graphite Nozzle
Out Side Dia. ( $d$ , inch)	2.125	2.125	2.125
Length ( $l_n$ , inch)	1.25	2.15	2.15
Throat Dia. ( $d_t$ , inch)	.245	0.30	0.33
Slope (Converging) Angle (degree), $\gamma$	45	30	30



1. Nozzle Cover
2. Exhaust Nozzle, Converging
3. Part of Pressure Chamber  
(Initial/Short Motor Pressure Chamber)  
Glass Windows Installed.
4. Pressure Chamber Extention
5. Head End Cover
6. Igniter

Figure 3.1 Modified Motor Component



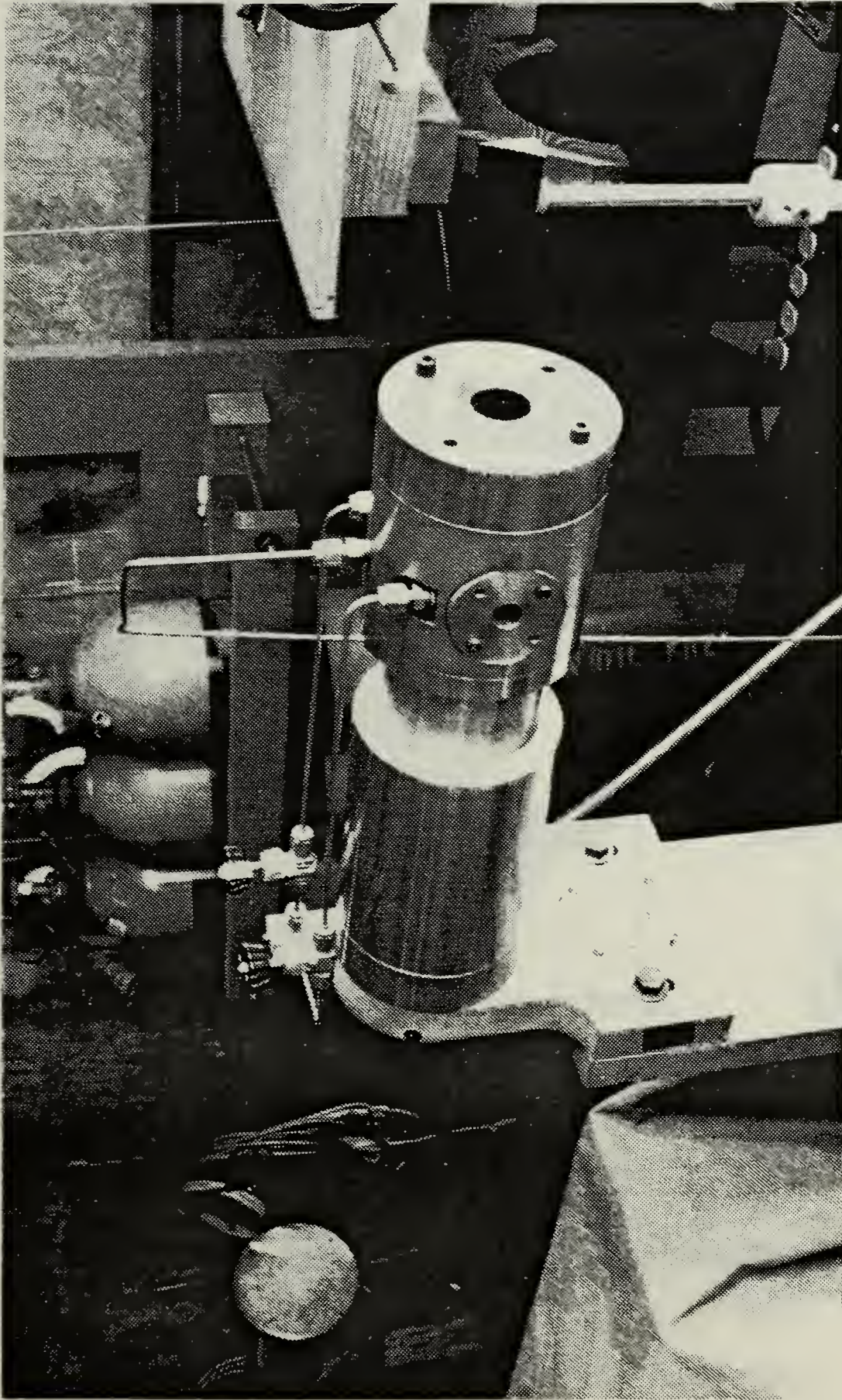


Figure 3.2 Installation of the Small Rocket Motor

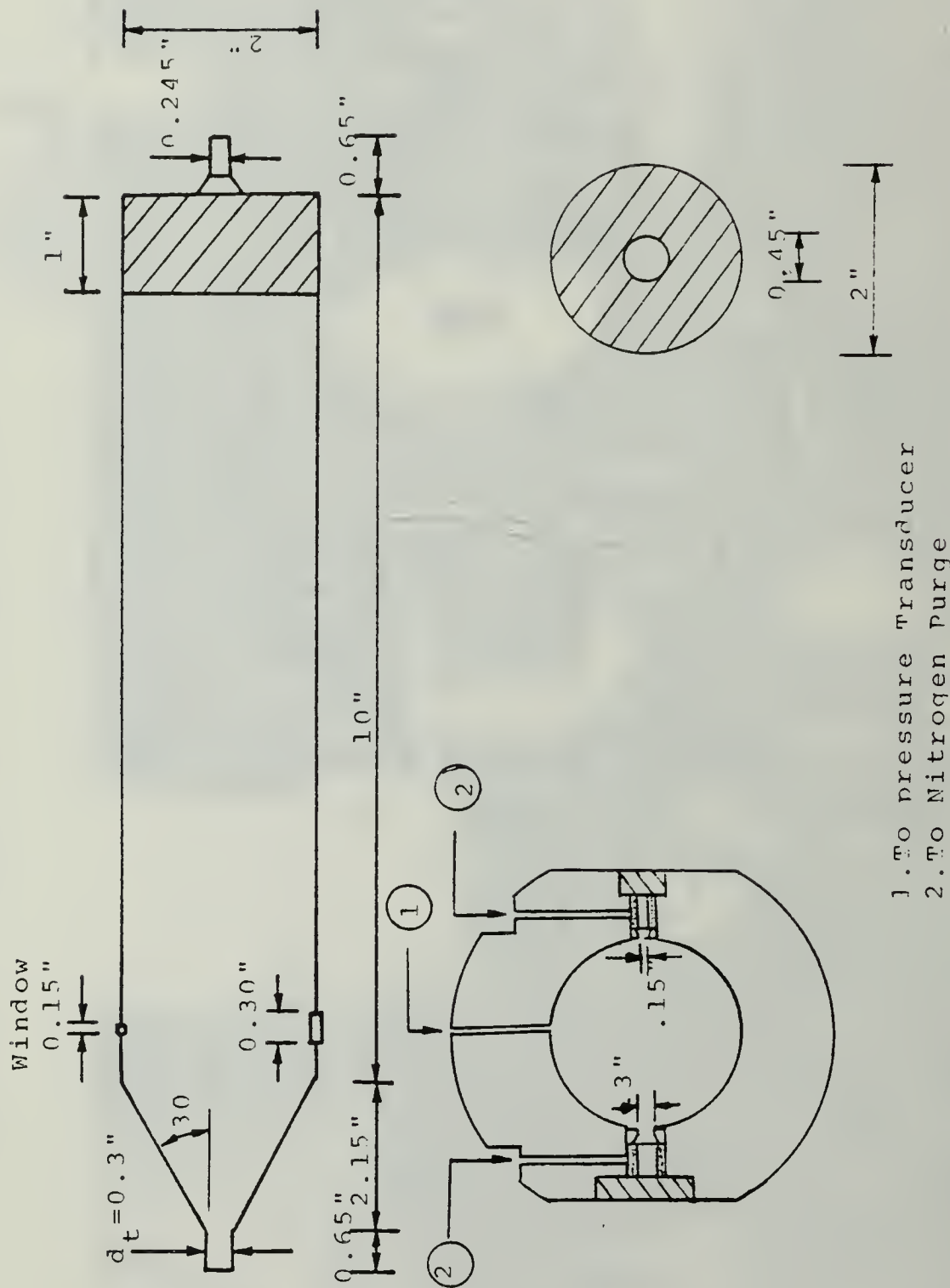


Figure 3.3 Schematic of the Short Motor



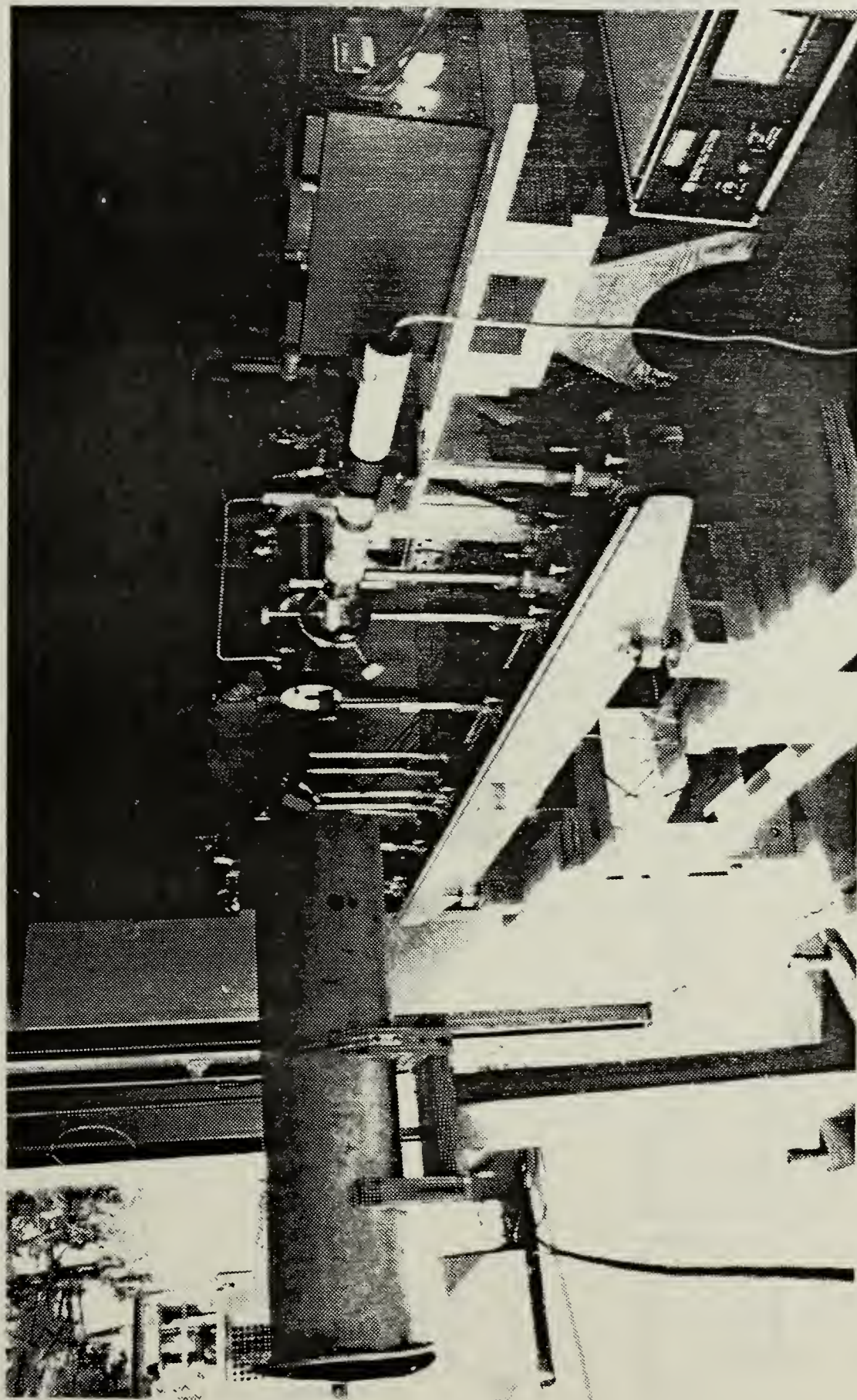


Figure 3.4 Photograph of Light Scattering Apparatus Set-up

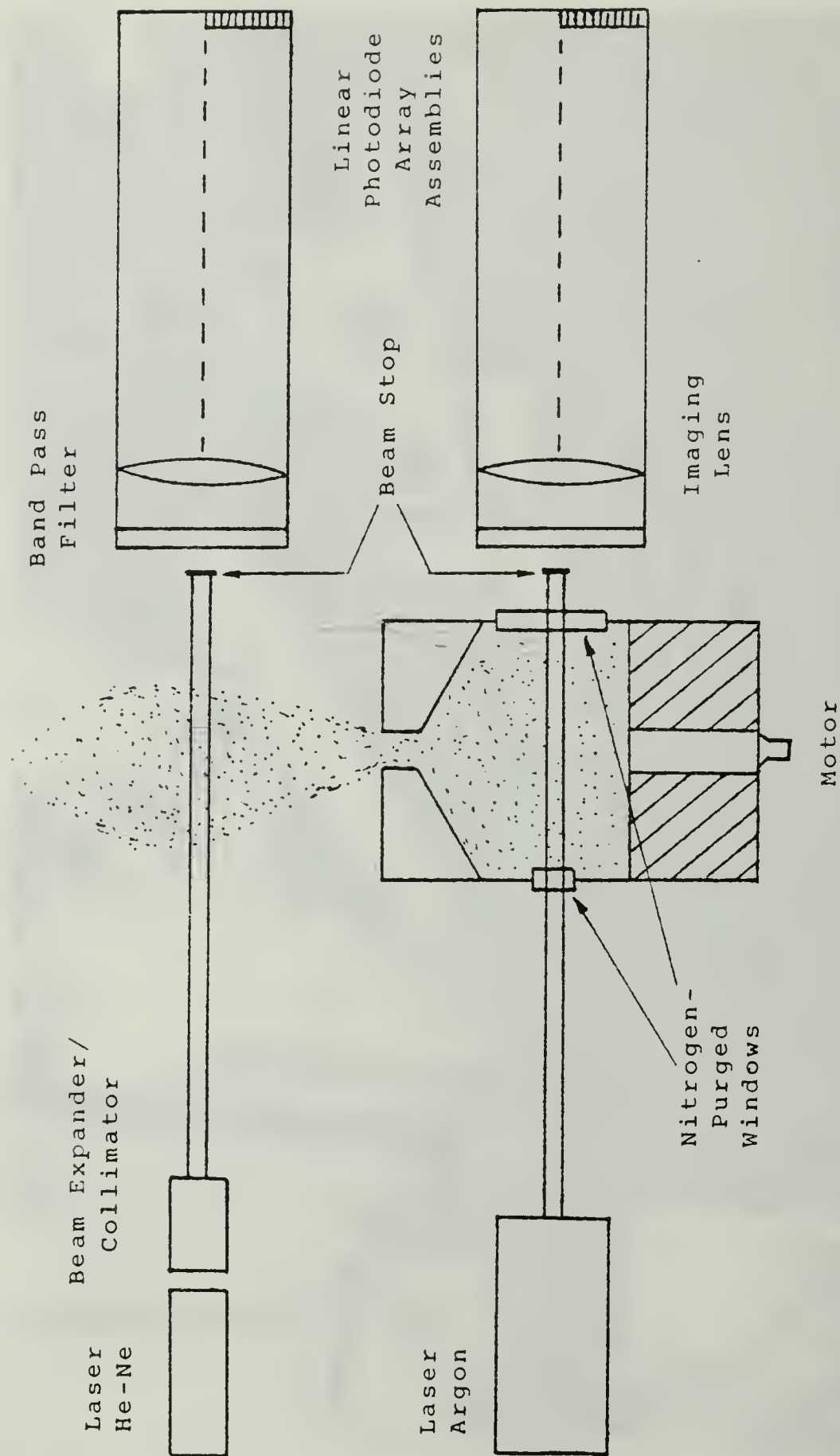


Figure 3.5 Schematic Diagram of Light Scattering Apparatus

TABLE II  
Light Source Specification

A. Argon Laser

1. Manufacturer	: Spectra-Physics
2. Model	: 162 - 03
3. Output Power	: 10 mWatt 488.0 nm or 5 mWatt 514.5 nm
4. Beam Divergence	: 1.0 rads full angle
5. Cavity Length	: 330 mm
6. Input Power Required:	10 Amperes at 117 VAC <u>± 10 W</u> , 50/60 Hz.

B. Helium-Neon Laser

1. Manufacturer	: Spectra-Physics
2. Model	: 147
3. Type	: He-Ne Class IIIB
4. Output Power	: 8 mWatt
5. Beam Diameter	: 0.92 mm
6. Beam Divergence	: 0.87 nrad.



#### IV. RESULT AND DISCUSSION

##### A. INTRODUCTION

The purpose of this investigation was to conduct solid rocket motor tests to determine the feasibility for obtaining particle size data across the exhaust nozzle using measurements of forward scattered laser light. If the technique is not only feasible, but also practical to utilize, then it could be used in conjunction with light transmission measurements at three wave-lengths to provide a valuable diagnostic tool. This diagnostic tool could then be used to obtain the much needed particulate size in exhaust nozzles as discussed in the Introduction. The apparatus had been previously developed and successfully calibrated using suspended particles without combustion. Application to the combustion environment remained to be done. In this investigation, three solid propellant composition were used with varying amounts of aluminium. Two of the propellant utilized a GAP binder with AP, one had no aluminium and the other used 4.8%, 20 micron aluminium. The third propellant was an HTPB/AP propellant with 2%, 40 micron aluminium and 0.25%  $\text{Fe}_2\text{O}_3$ . Initial tests were conducted using a short motor cavity length. Difficulties arose which required using a longer motor cavity length for all subsequent test.

##### B. EXPERIMENTS USING THE SHORT MOTOR CAVITY LENGTH

In solid propellant motors agglomerate size may depend on many factors such as the propellant type, original particle size, chamber pressure, burning rate, aluminum concentration and motor geometry. Short residence times can lead to poor combustion efficiency. The tests conducted

using the short motor are summarized in Table III, which indicates the residence time was less than 3 millisecond. For good combustion efficiency (the conversion of all aluminium to aluminium oxide), typical minimum residence times are between 10 and 15 milliseconds. It was apparent from examination of the exhaust nozzle after a firing that large agglomerates of aluminium/aluminium oxide were impinging on the converging surface of the exhaust nozzle. This also resulted in large particles exhausting through the nozzle exit.  $D_{32}$  from the measurements was approximately 50 microns (Figure 4.1). SEM photographs (Figure 4.2) indicated particles ranging from the one micron size up to 60 microns. It was therefore decided to lengthen the motor to increase residence time to between 10 and 15 milliseconds without adding additional propellant. This required an eight inch extension onto the initial two-inch length. Table IV indicates that the residence time was usually increased to between 10 and 15 milliseconds. Initial tests using this motor indicated that the nozzle impingement problem was eliminated.

### C. SYSTEM CALIBRATION

Although the apparatus had been previously calibrated by Harris [Ref. 21] it was necessary to determine the maximum attenuation of the transmitted beam which allowed the scattering measurements to be made. As discussed above, single scattering generally requires transmittances greater than 90%. Calibrations were therefore conducted using 37 - 44 micron glass beads suspended in water. Tests were conducted with transmittances of 82%, 55%, and 29%. The results are presented in Figures 4.3 to 4.8. When the highest transmittance of 82% was used, both the curve fit and two-angle ratio methods resulted in good agreement (45 microns) with



the actual particle size. As the transmittance was decreased to 55% and 29%, the measured sizes decreased to 42 and 36 microns respectively. In addition the two-angle method did not yield good results for the lower transmittances.

These results indicate that the scattering measurements can be used to determine particle size when the transmittance is significantly less than 90%. A test was then conducted to determine the exhaust opacity with no aluminium present. This was necessary to determine the extent of attenuation caused by such things as condensed soot and refraction caused by thermal gradients. The test was conducted as follow :

1. The transmitted beam was centered on the diode array. Data were taken with the beam blocked and then unblock to obtain the intensity profile using the apparatus which is set up to obtain pre-firing and firing data.
2. The motor was then fired using the standard sequence. The beam was blocked for obtaining zero data and then data was taken on firing the motor. The results are shown in Figure 4.9. A 55% attenuation of the transmitted beam occurred. The position of the beam peak intensity was observed to be the same, indicating no preferred refraction. The Gaussian was broadened, apparently by scattering. These results indicated that scattering measurements made with aluminium oxide present could be difficult to interpret. The small angle scattering (beam broadening) is not as much a concern as the beam attenuation, since larger scattering angles are used to measure the small  $\text{Al}_2\text{O}_3$  particles. A similar test was also conducted with the non-metalized propellant in which the nozzle entrance beam was monitored. During this test the transmitted beam was deflected off of the diode array. The beam also shifted on the diode used to measure the

transmitted light. It was attenuated by approximately 80%, but it is not clear whether this was due to soot/smoke and/or to the beam shift. Examination of the apparatus revealed the cause for the shift of the beam. The laser beam was not perfectly aligned with the windows, resulting in refraction at the window-motor cavity interface. When the motor was fired the refractive index of the gases changed, resulting in a beam movement. This points out the need for very careful alignment of the nozzle entrance optics.

#### D. NOZZLE EXHAUST MEASUREMENTS

Two tests were conducted using non-metalized propellant. The results from the two runs were almost identical. Results from one of the tests are presented Figure 4.10 and 4.11. Significant scattering was apparent to angles of 0.018 radians. This was even more severe than observed in the test discussed above. It is not clear exactly what caused this small angle scattering. One possibility is beam movement/broadening to the extent that it can diffract around the edges of the beam stop. These results indicate that measurements made with this propellant system which also contains aluminium can only be done for angles greater than approximately .018 radians.

Two tests were then conducted with the GAP propellant containing 4.8% aluminium. Again the results were repetitive. Figure 4.12 shows that for the "allowable" angles greater than 0.018 radians (diode number 375), the voltage level was approximately four times greater than the voltage without aluminum (figure 4.11). Use of iterative graphics to determine  $D_{32}$  by the curve fitting method (Figure 4.13) or using the two angle method (Figure 4.14) resulted in a measured

size between 6 and 7 microns. Examination of the collected exhaust using the SEM (Figure 4.15) showed a range in particle sizes. Most of the particles were within the range of 0.5 to 1.5 microns, some were 5 microns, and a few were 7.5 microns. These results are in reasonable agreement with the measured results since the optical method has a strong bias toward the large particles.

Three tests were then conducted using the propellant with 2% aluminium. The results were again repetitive. Results from one run are presented in Figures 4.16 and 4.17. A  $D_{32}$  of 5.5 micron was obtained by the curve fit method, and 8 to 9 microns was obtained by the two angle method. SEM examination of collected exhaust showed (Figure 4.18) particles as large as 15 to 20 microns, a few between 5 and 10 microns, and many in the one micron range. The larger particles may be due to unburned aluminium (original powder size was 40 micron).

#### E. NOZZLE ENTRANCE MEASUREMENTS

These data were actually obtained during the same tests that the nozzle exhaust measurements were made. The data were quite repetitive from multiple runs. Experiments using the non-metalized solid propellant resulted in diode saturation at angles less than 0.016 radians, which corresponded to diode number 384. It is not known at this point whether the beam shift was due to optical misalignment or to thermal gradients. However, if scattering measurements are to be made using the metalized propellants, the data must only be considered for scattering angles greater than 0.02 radians (or correspondingly, to diode numbers greater than 500), Figures 4.19 and 4.20 show these results.

Figure 4.21 shows the results obtained using the propellant with 4.8% aluminium. Unfortunately, the useable data

from diode 500 to diode 576 did not allow any particle data to be obtained. SEM examination of the collected exhaust showed some particles in the 4 to 8 micron range, and many in the 0.5 to 1 micron range. A photograph of this sample is presented in Figure 4.22.

The results obtained with the solid propellant with 2% aluminium are shown in Figures 4.23 and 4.24. The data appear to have much less transmitted beam effects than the 4.8% aluminized propellant. The intensities were too low to use the curve fit method for theta ( $\theta$ ) greater 0.02 radians. The two-angle method resulted in a  $D_{32}$  of approximately 8 microns. SEM evaluation showed particles in the 9 to 10 micron range, but with many less than 3 microns (Figure 4.25).



TABLE III  
Experimental Results from Short Motor

Date of Test	Weight Percent of Aluminum	Pressure Pc (Psig)	Burning Time (sec.)	Residence Time (msec.)
Jun 8, 84	4.8	440	1.05	2.3
Jly 27, 84	2.0	220	2.03	1.1
Aug 21, 84	4.8	680	0.55	2.0
Aug 23, 84	4.8	435	1.05	2.3
Sept 18, 84	4.8	300	2.3	3.4
Dec 2 , 84	4.8	240	1.55	2.0
Dec 28, 84	4.8	285	1.6	2.3
Jan 8, 85	4.8	255	2.1	2.7

Note :

Propellant density 4.8 % Al =  $0.065 \text{ lbs/in}^3$

2 % Al =  $0.062 \text{ lbs/in}^3$

Temperature = 6100 deg. R

CURVE FIT RESULTS  
INTENSITY VS. THETA

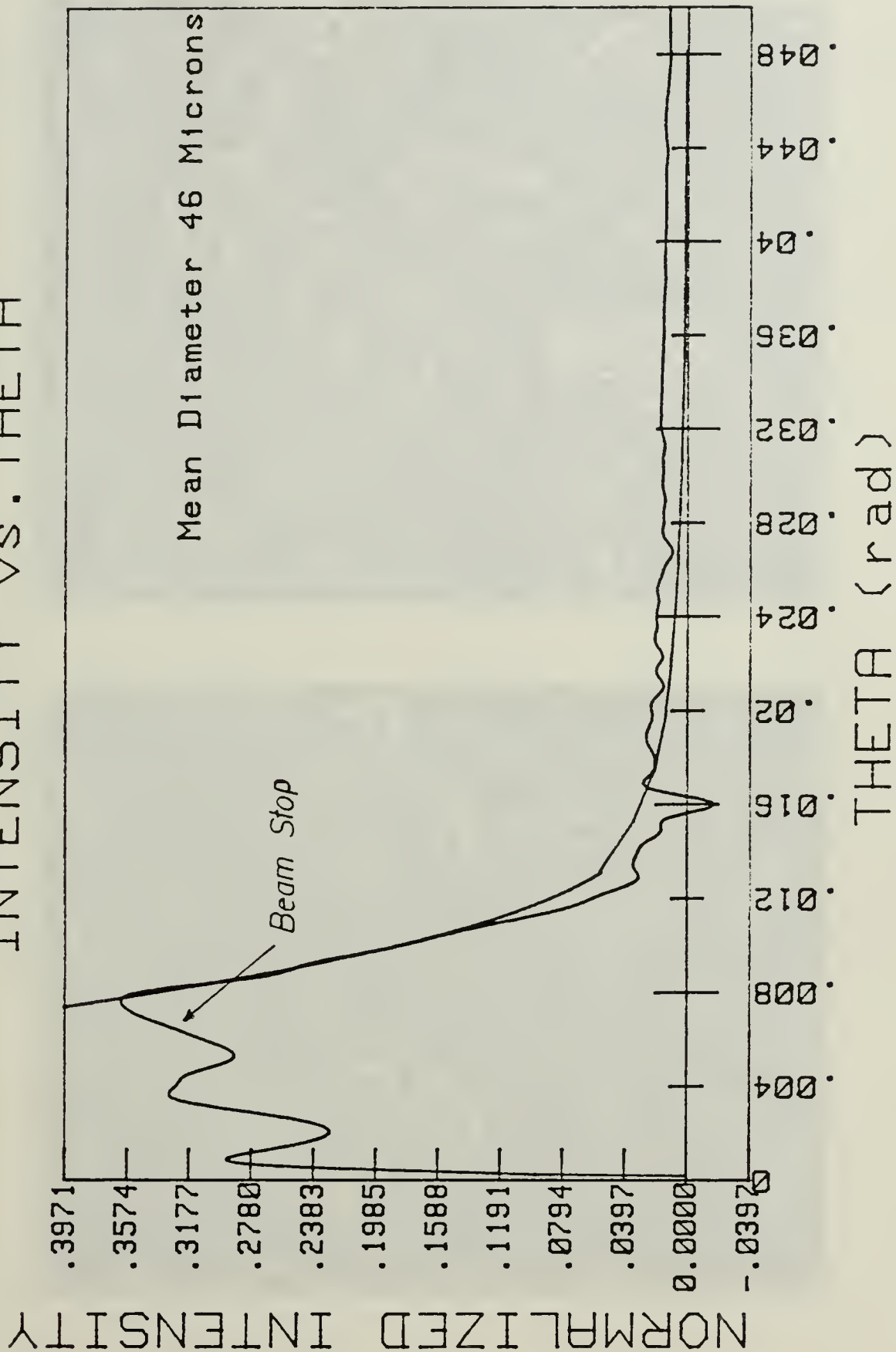


Figure 4.1 D Results by Curve Fit Method



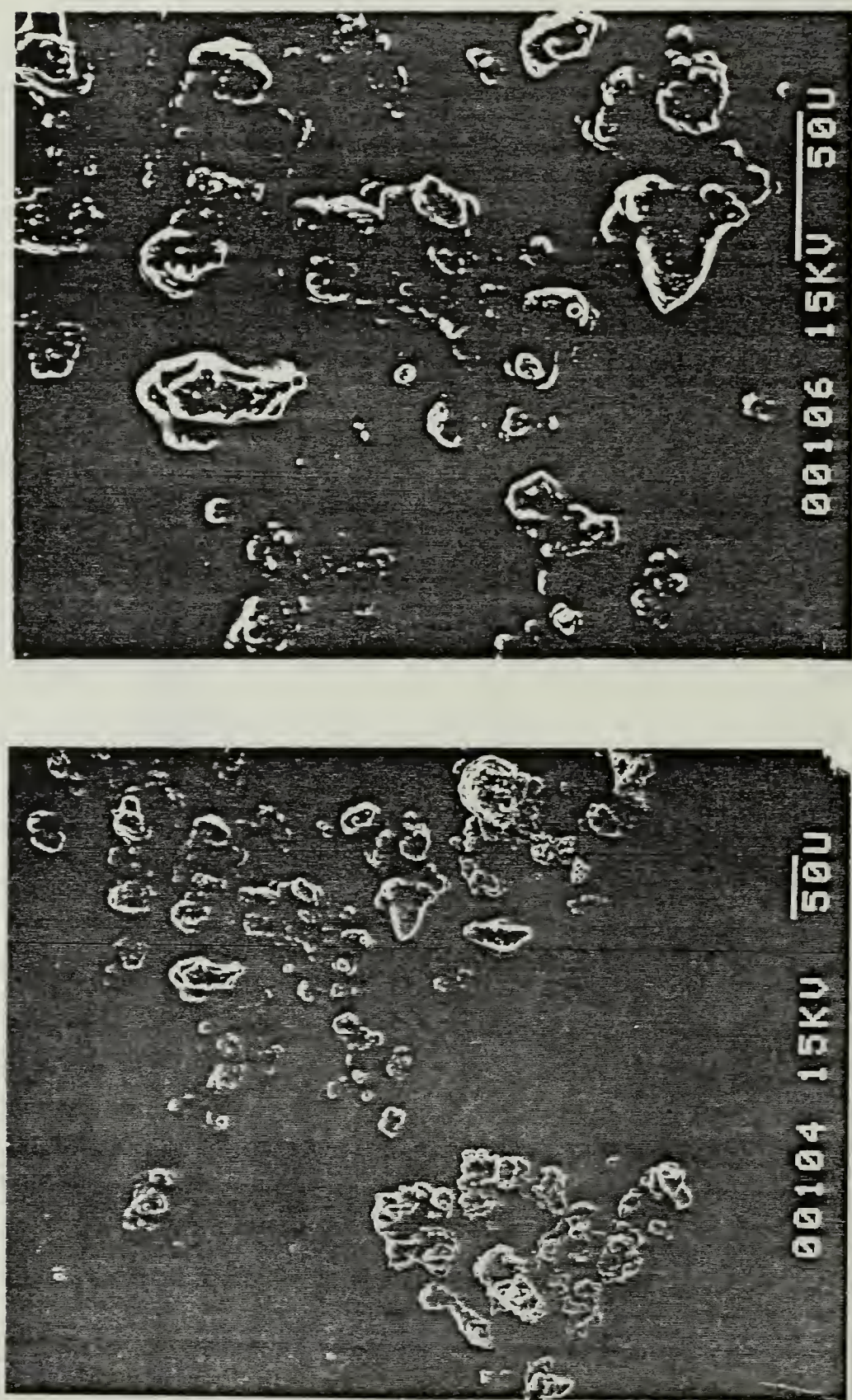


Figure 4.2 SEM Evaluation, 4.8% Al Propellant Short Motor

TABLE IV  
Experimental Results from Long Motor

Date of Test	Weight Percent of Aluminum	Pressure Pc (Psig)	Burning Time (sec.)	Residence Time (msec.)
Jan 18, 85	4.8	298	2.7	14.5
Feb 1, 85	4.8	247	2.5	11.1
Feb 4, 85	0	257	1.4	6.3
Feb 12, 85	4.8	176	2.5	7.9
Feb 13, 85	4.8	235	2.3	9.7
Feb 14, 85	0	500	1.5	13.1
Feb 15, 85	0	192	1.5	5.0
Feb 20, 85	2.0	182	3.6	12.1
Feb 21, 85	2.0	142	3.6	9.6
Feb 28, 85	2.0	115	3.7	11.5
Mar 11, 85	0	360	1.1	7.9

Note :

Propellant density and Temperature

Calculation the same with in Table III

# CURVE FIT RESULTS INTENSITY vs. THETA

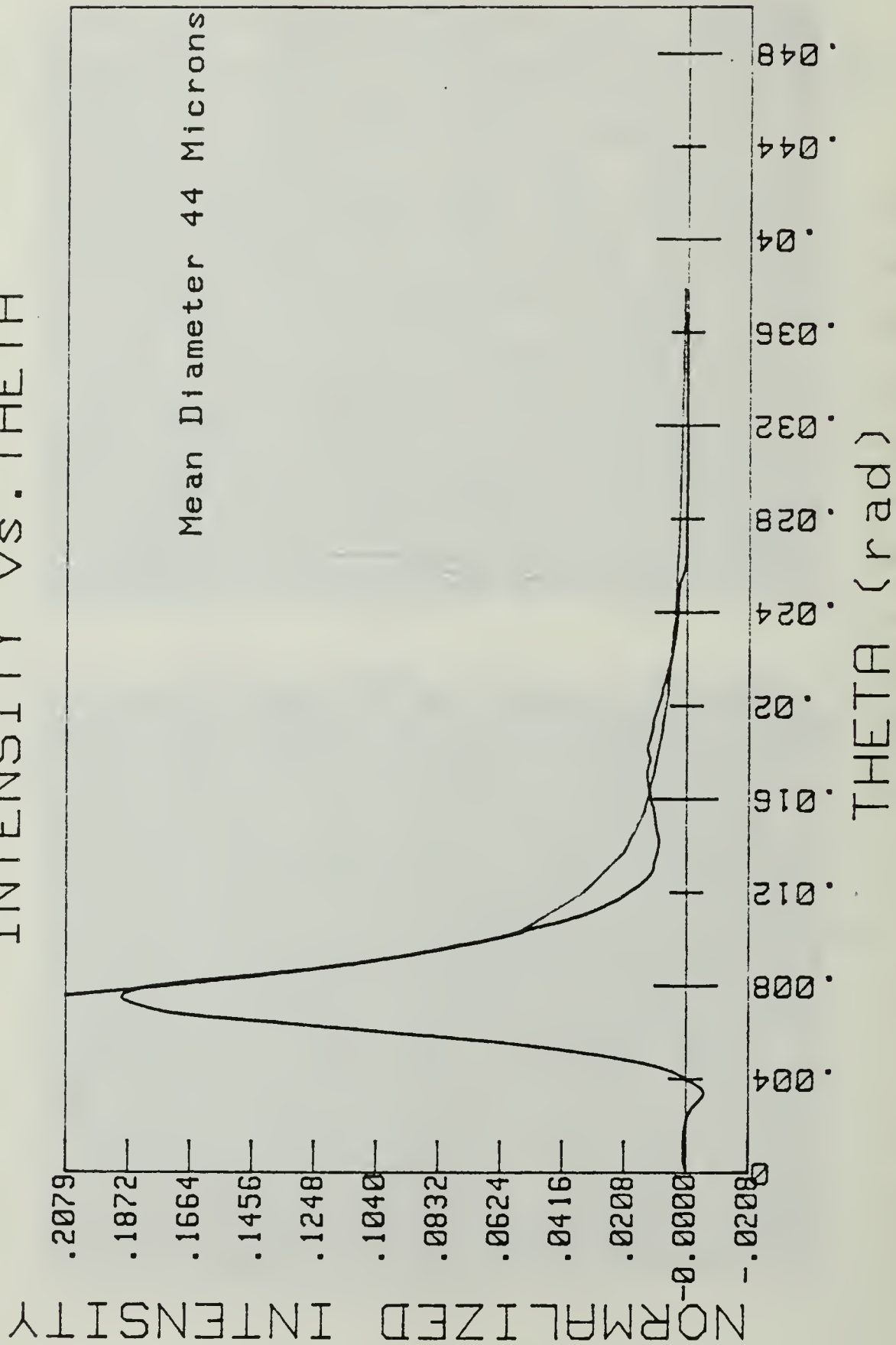


Figure 4.3 Curve Fit Method Using 82% Transmitted Light



# CURVE FIT RESULTS INTENSITY VS. THETA

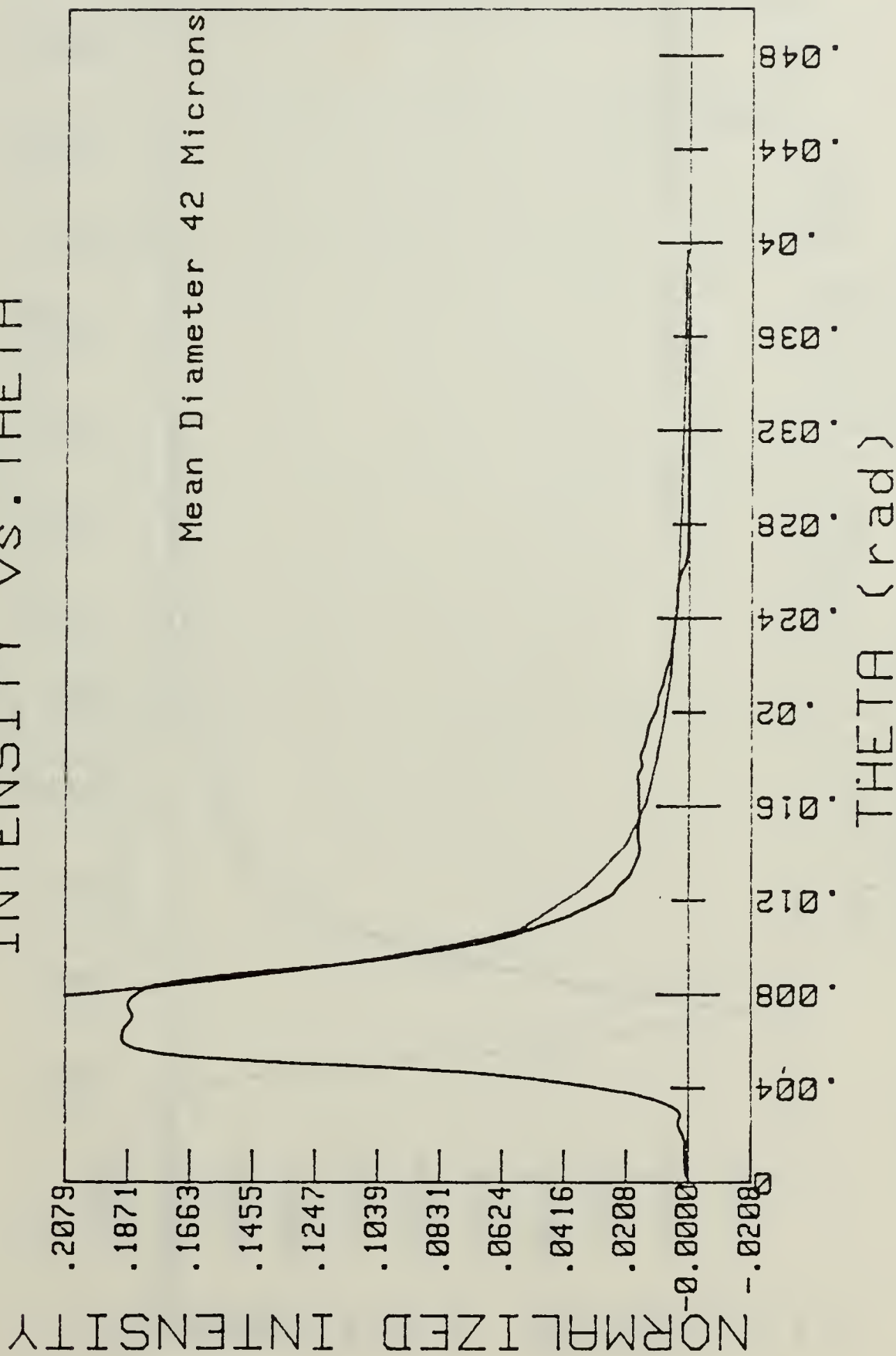


Figure 4.4 Curve Fit Method Using 55% Transmitted Light

# CURVE FIT RESULTS INTENSITY vs. THETA

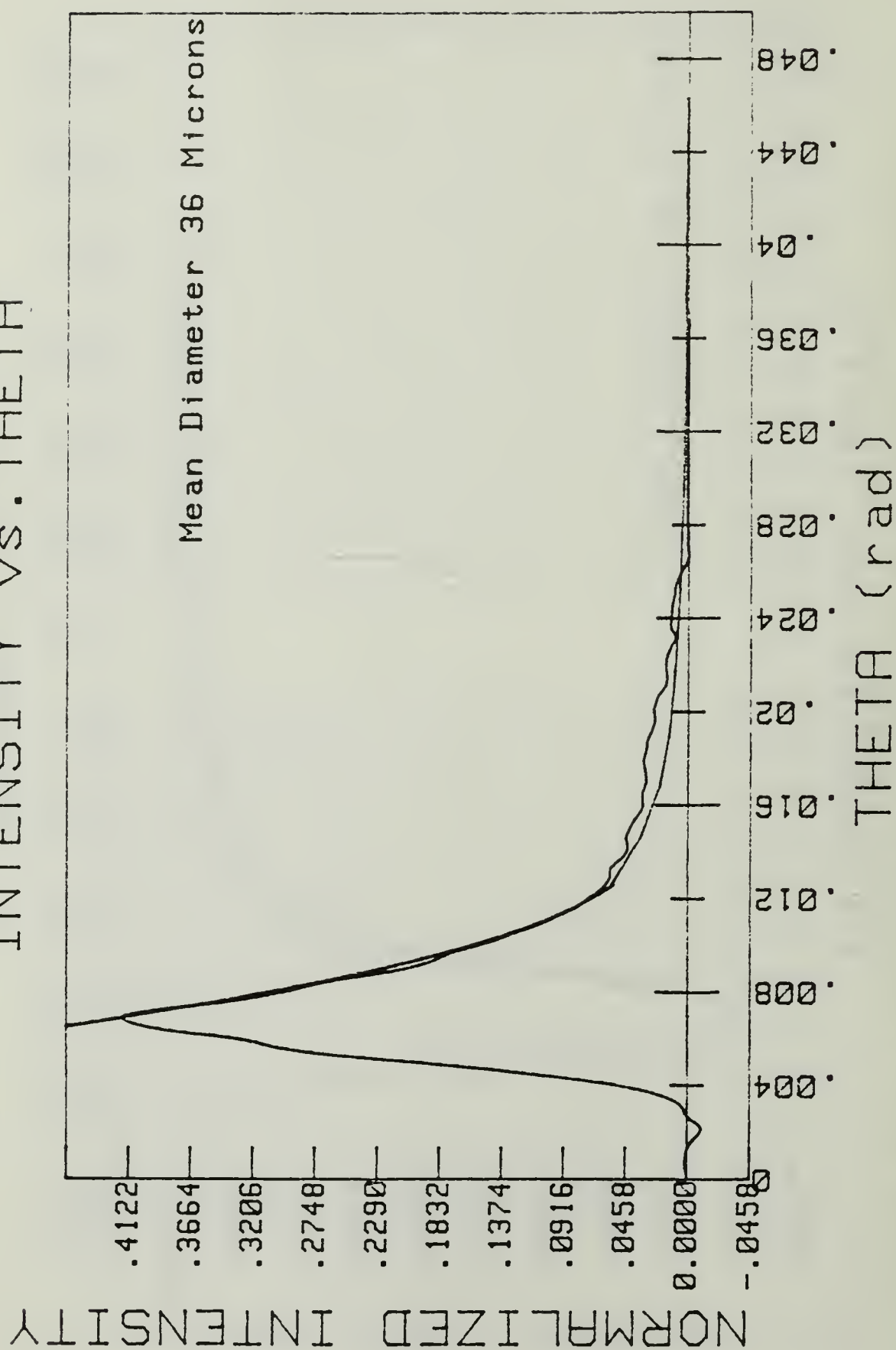


Figure 4.5 Curve Fit Method Using 29% Transmitted Light

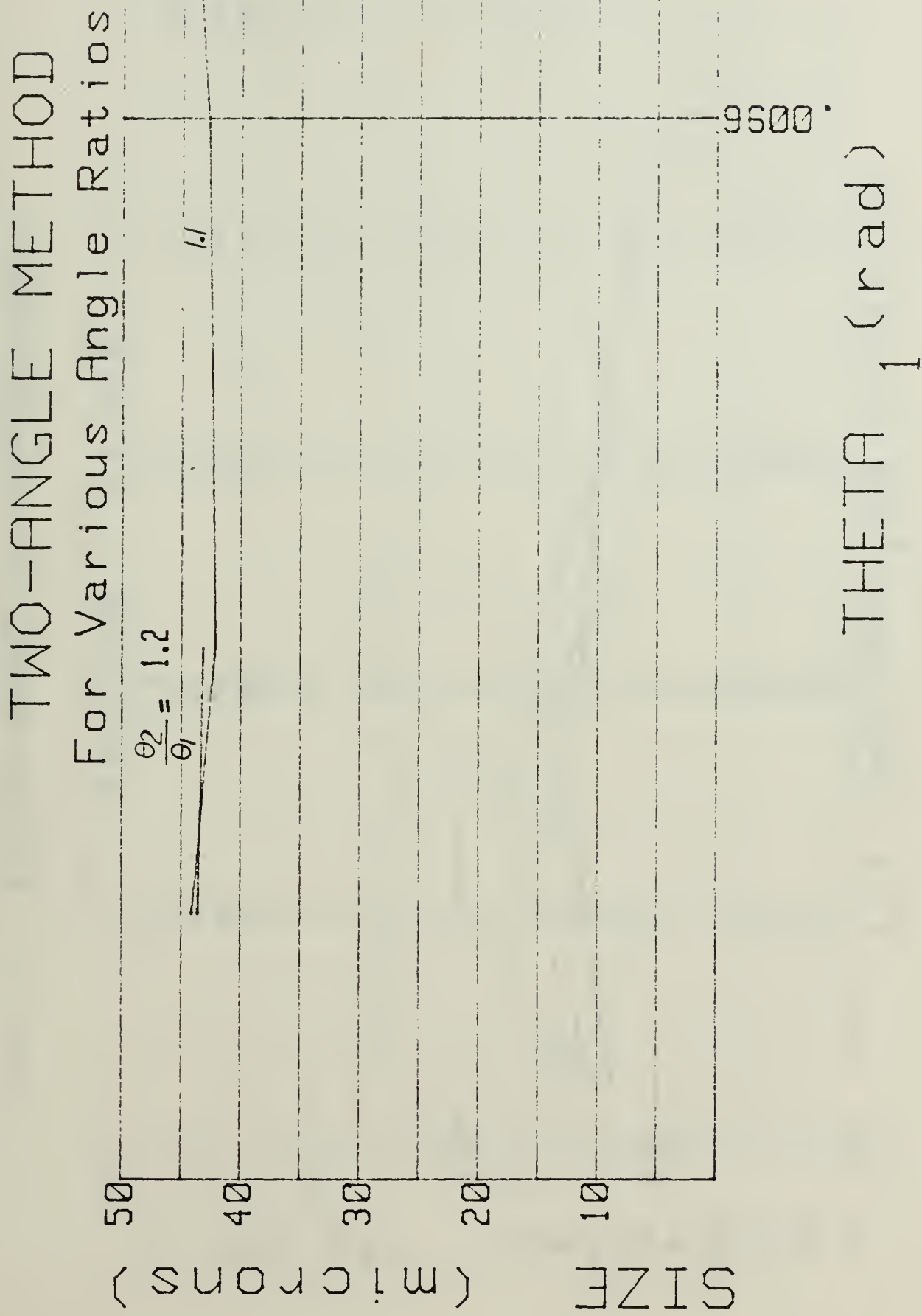


Figure 4.6 Two Angle Method Using 82% Transmitted Light



# TWO-ANGLE METHOD

For Various Angle Ratios

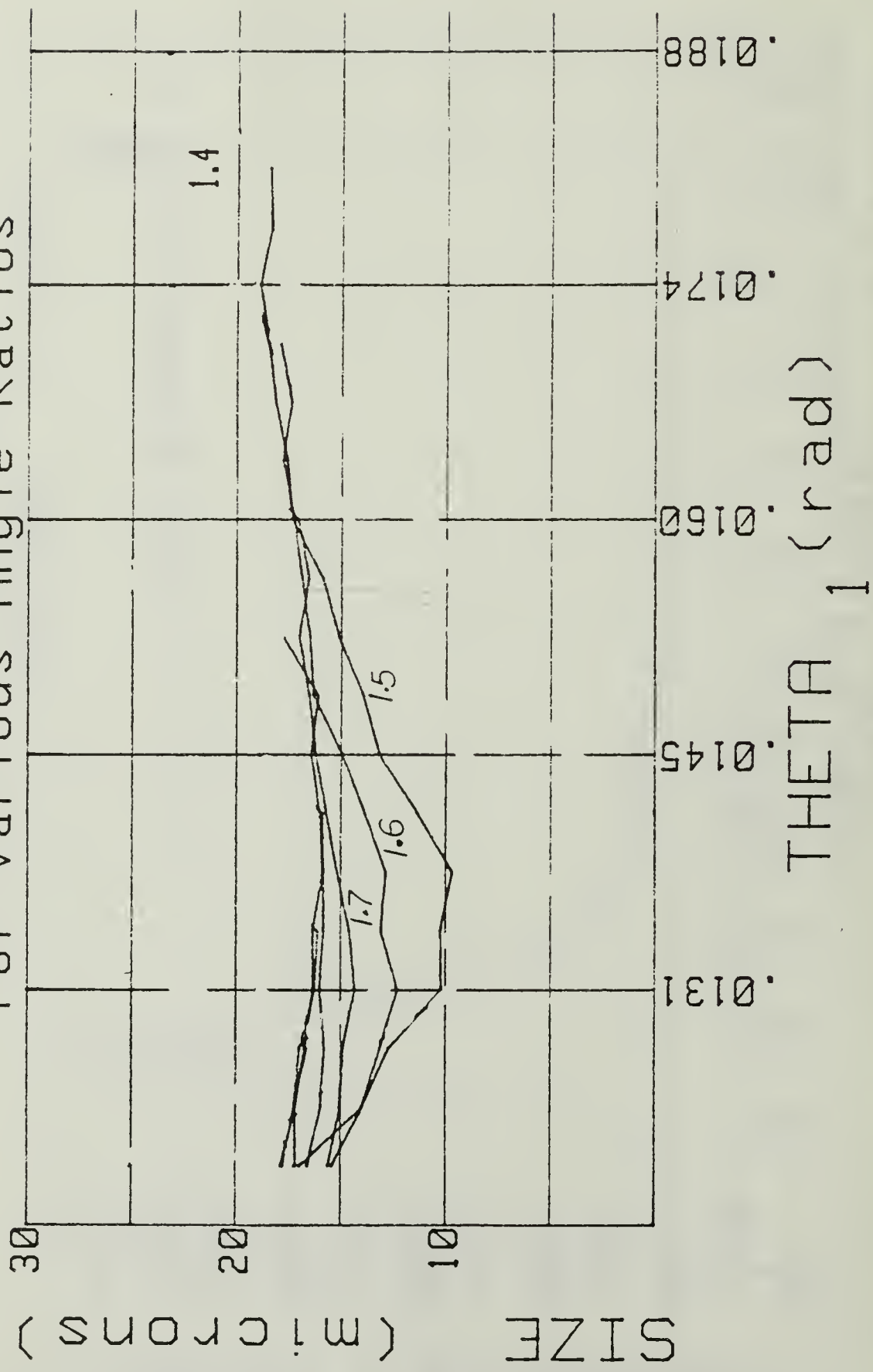


Figure 4.7 Two Angle Method, 55% Transmitted Light

# TWO-ANGLE METHOD For Various Angle Ratios

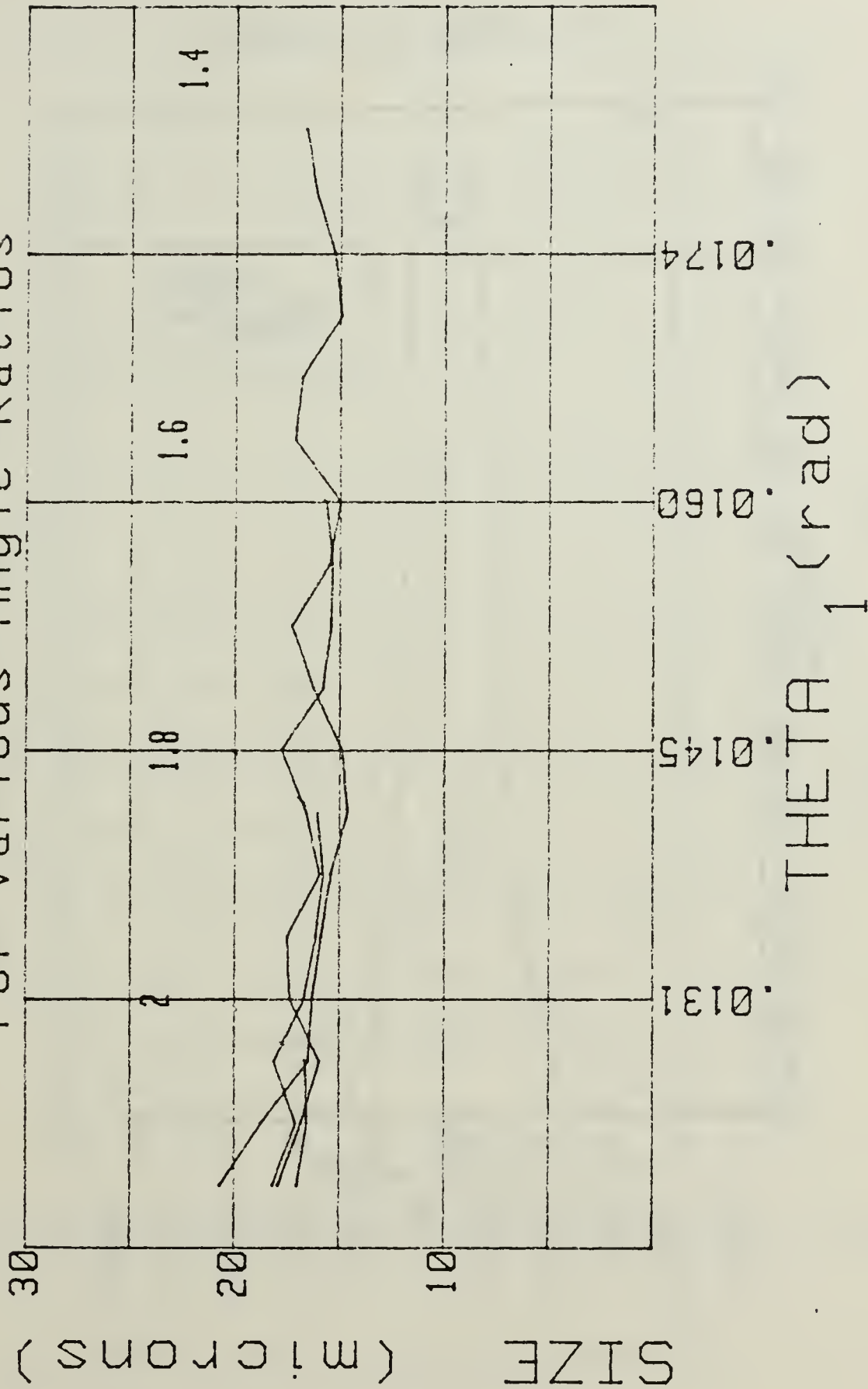


Figure 4.8 Two Angle Method Using 29% Transmitted Light

## VOLTAGE VS DIODE

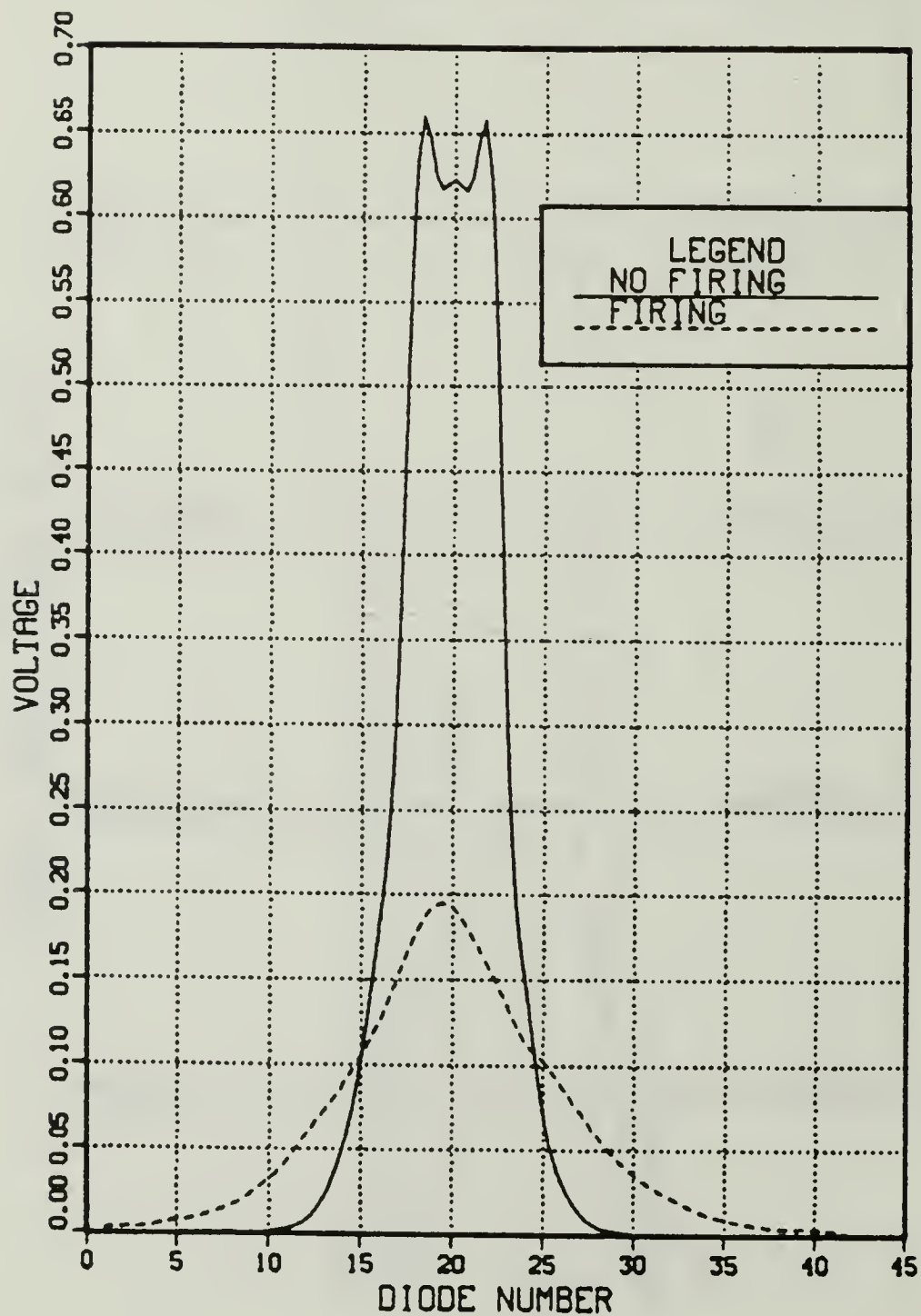


Figure 4.9 Non-metalized Propellant, 55% Attenuation

# CURVE FIT RESULTS INTENSITY vs. THETA

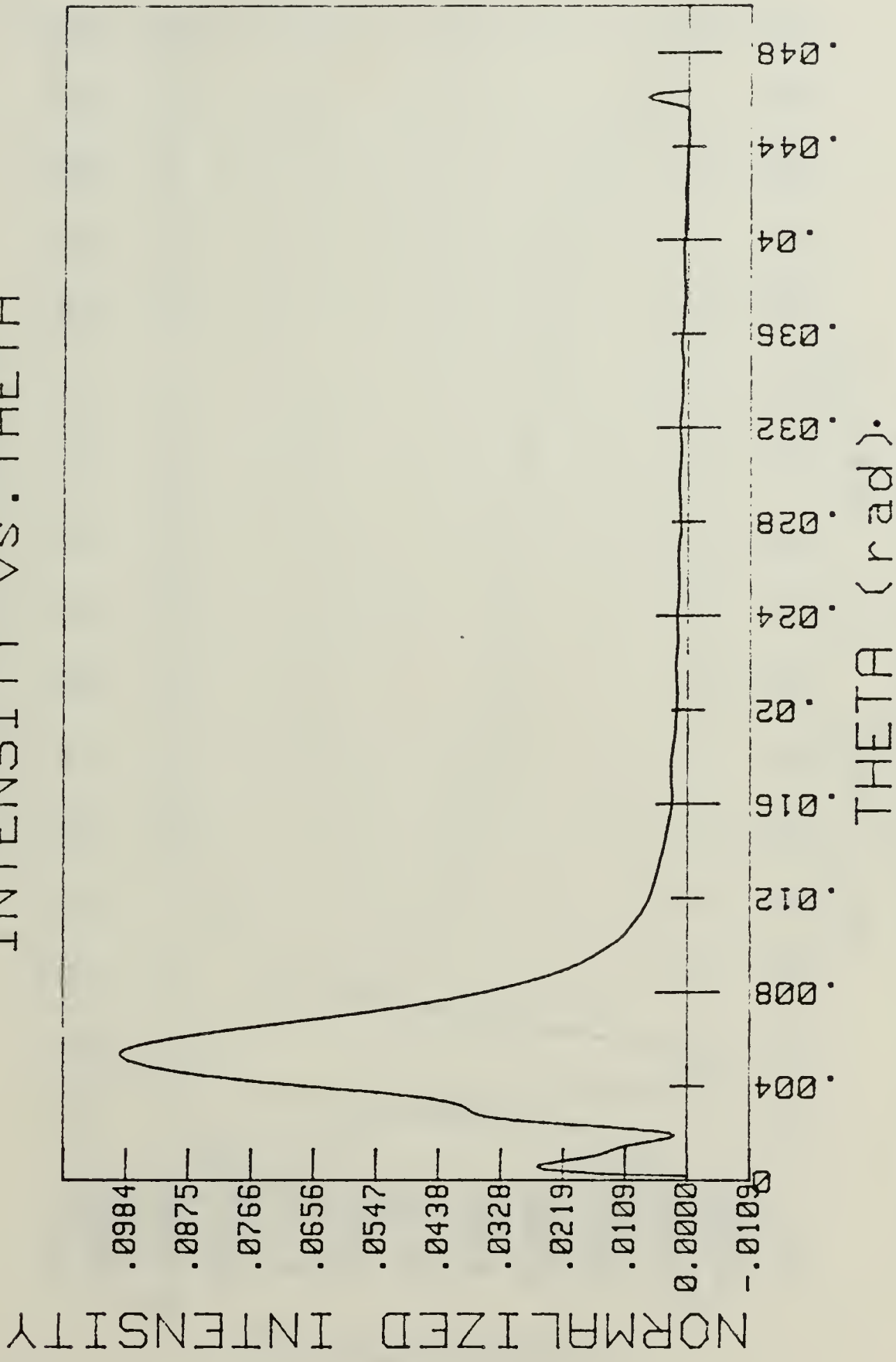


Figure 4.10  $I(\theta)$  vs Theta ( $\theta$ ), Non-Metalized Propellant

# FILTERED DATA VOLTAGE vs. DIODE

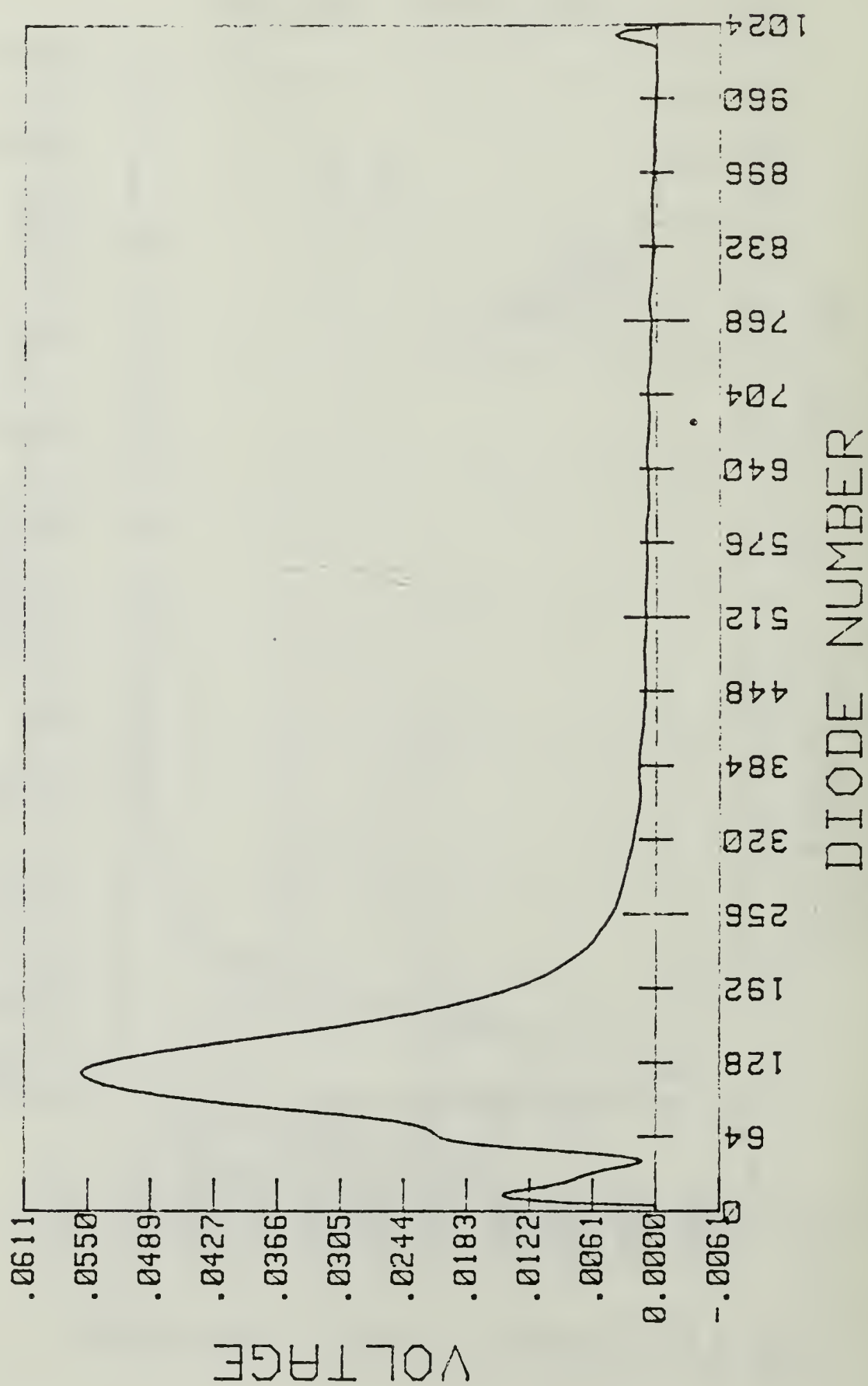


Figure 4.11 Voltage vs Diode, Non-Metalized Propellant

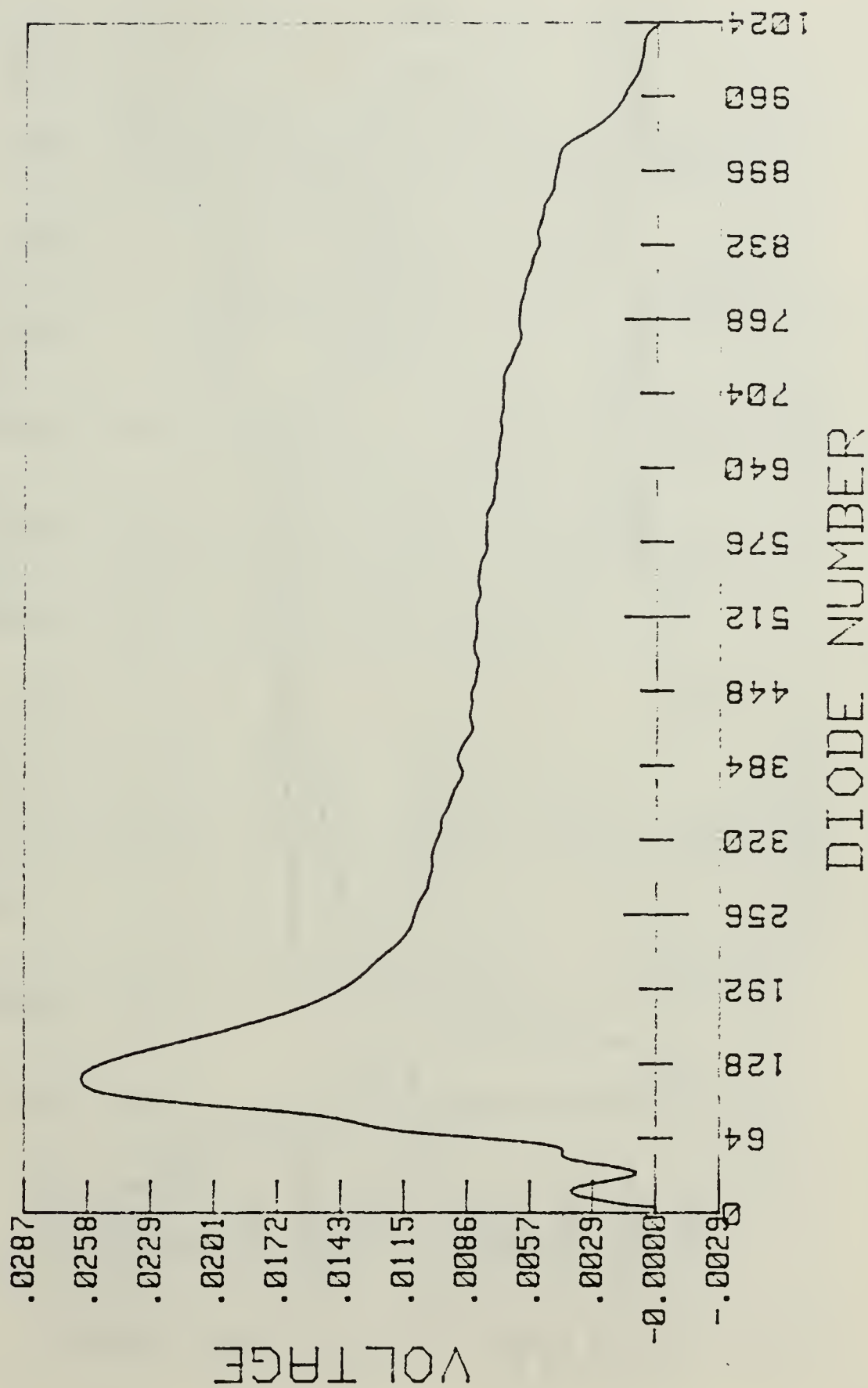


Figure 4.12 Voltage vs Diode, 4.8% Aluminum Propellant



# CURVE FIT RESULTS INTENSITY vs. THETA

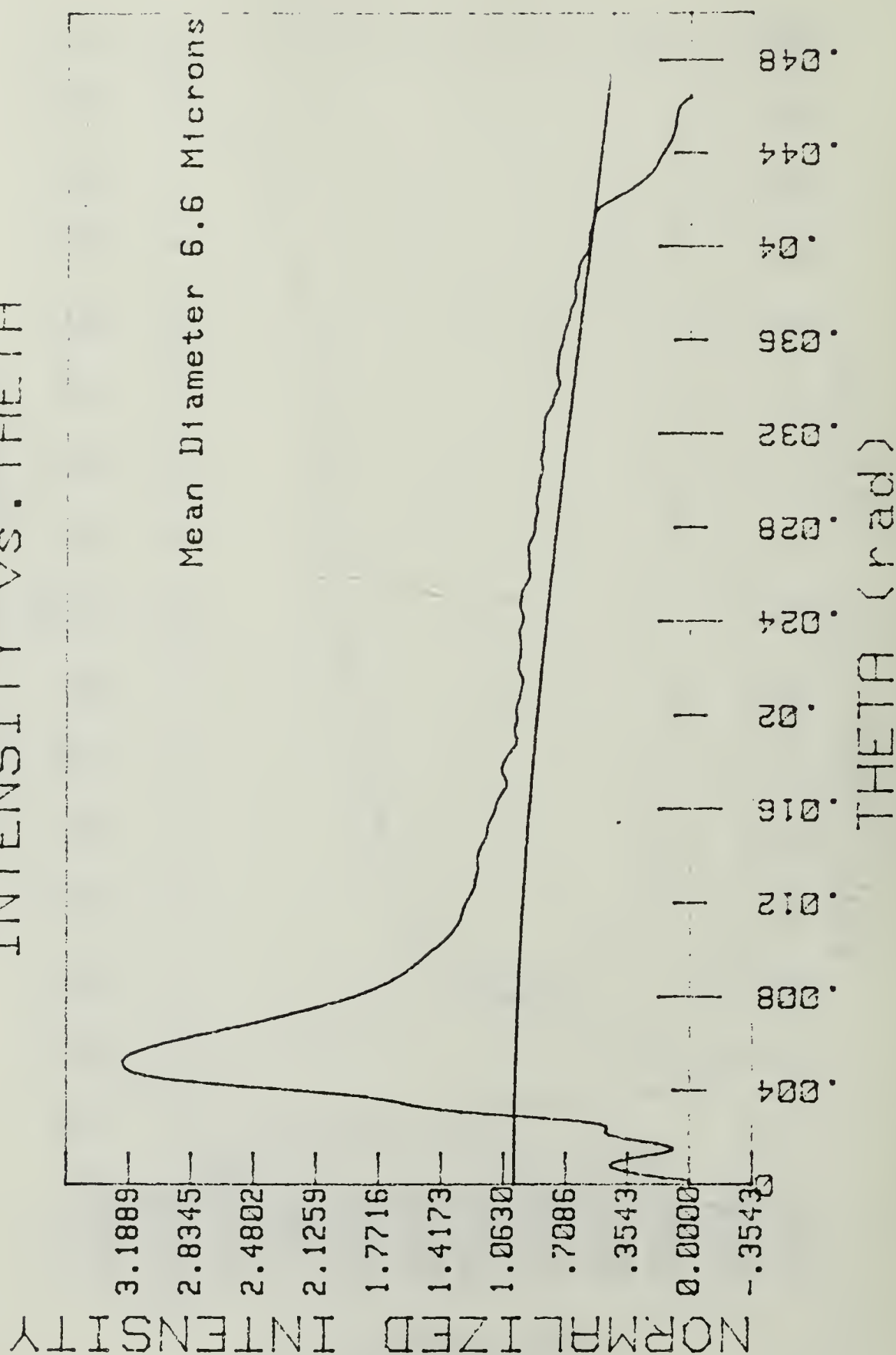


Figure 4.13  $I(\theta)$  vs Theta ( $\theta$ ), 4.8% Aluminum Propellant

TWO-ANGLE METHOD

For Various Angle Ratios

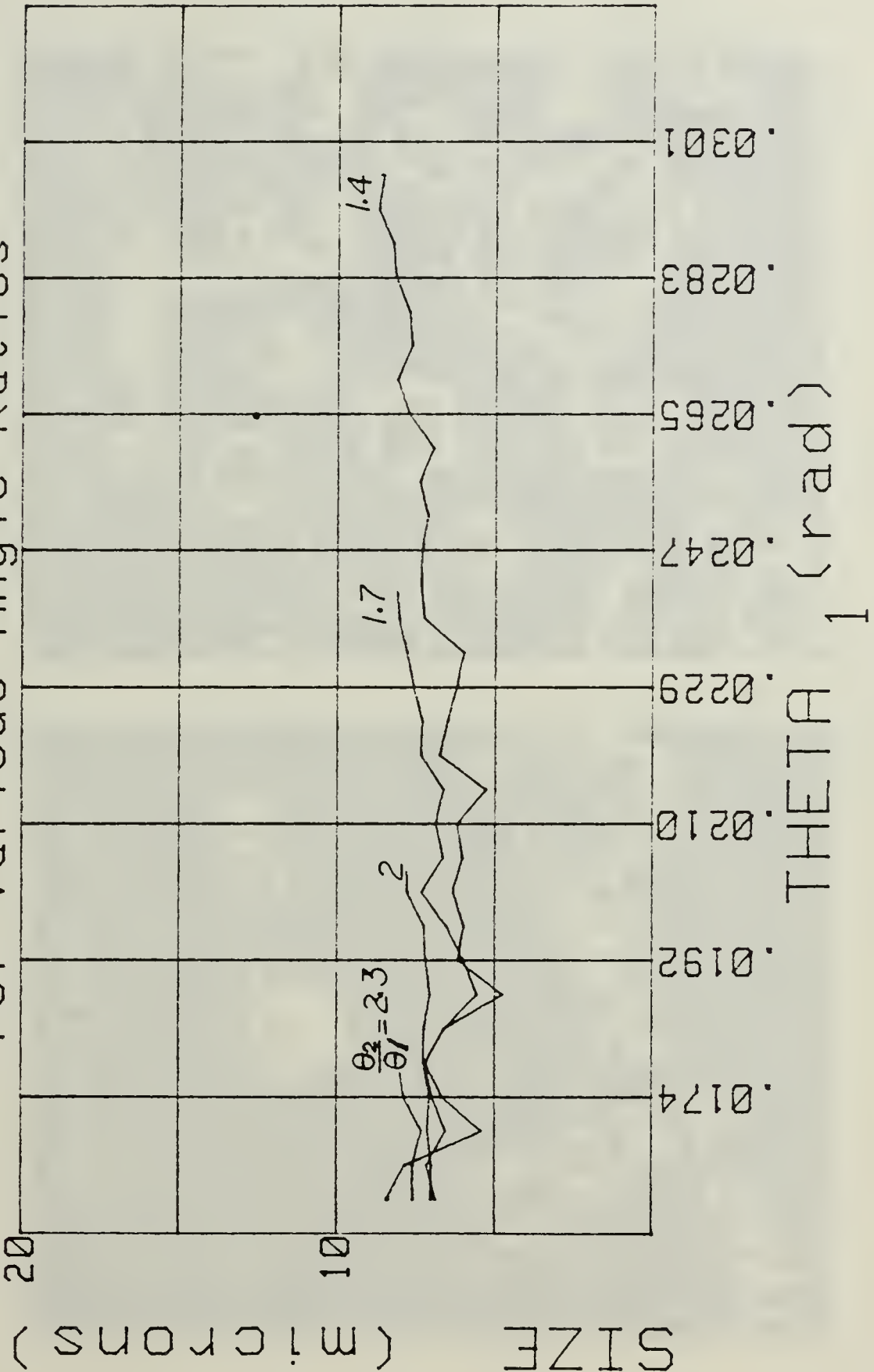


Figure 4.14 Two-Angle Method, 4.8% Aluminum Propellant, Exhaust



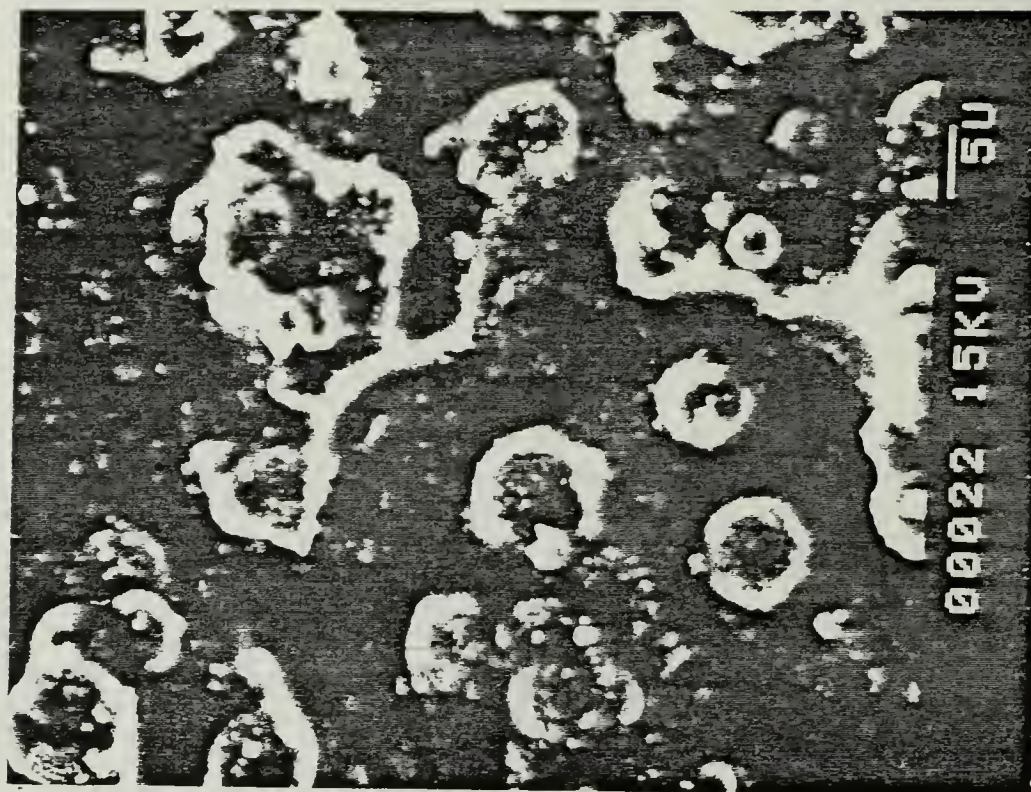
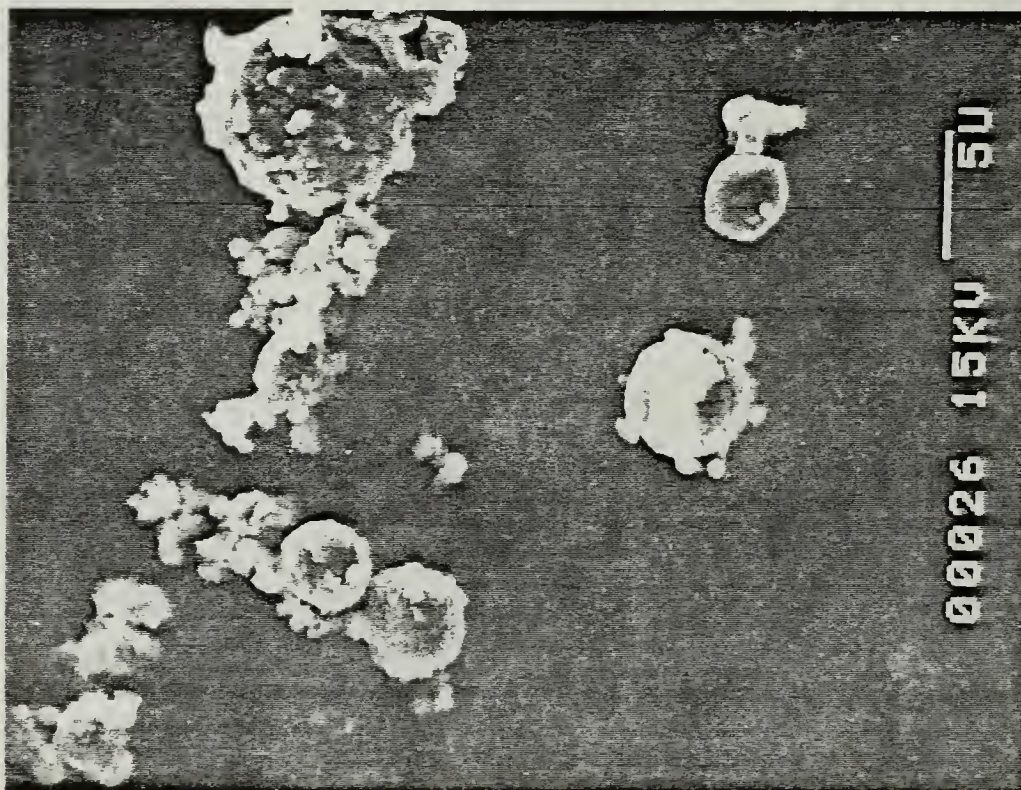


Figure 4.15 Collected Exhaust Particle, 4.8% Aluminum Propellant

CURVE FIT RESULTS  
INTENSITY VS. THETA

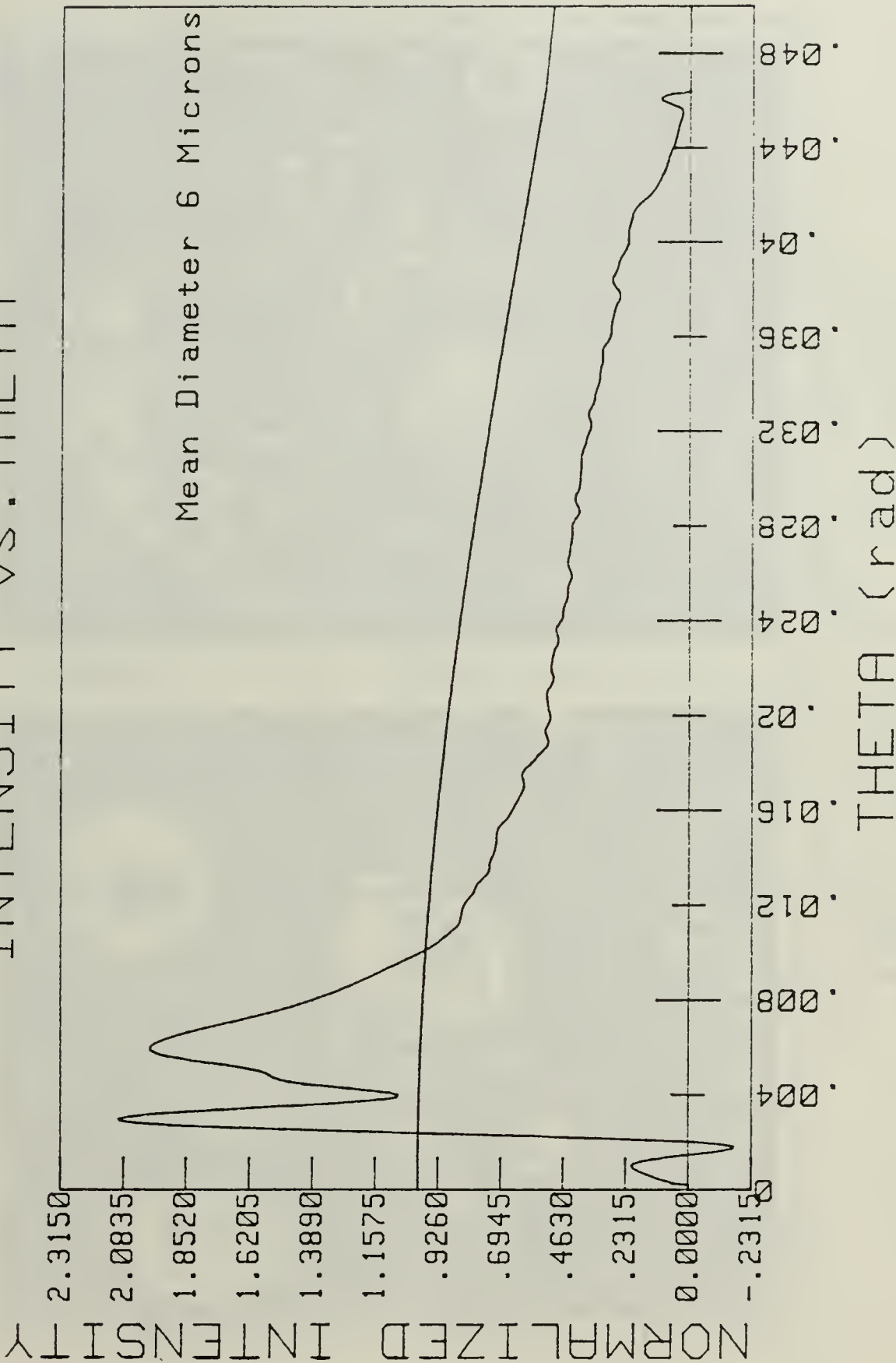


Figure 4.16 Curve Fit Method, 2% Aluminum Propellant, Exhaust



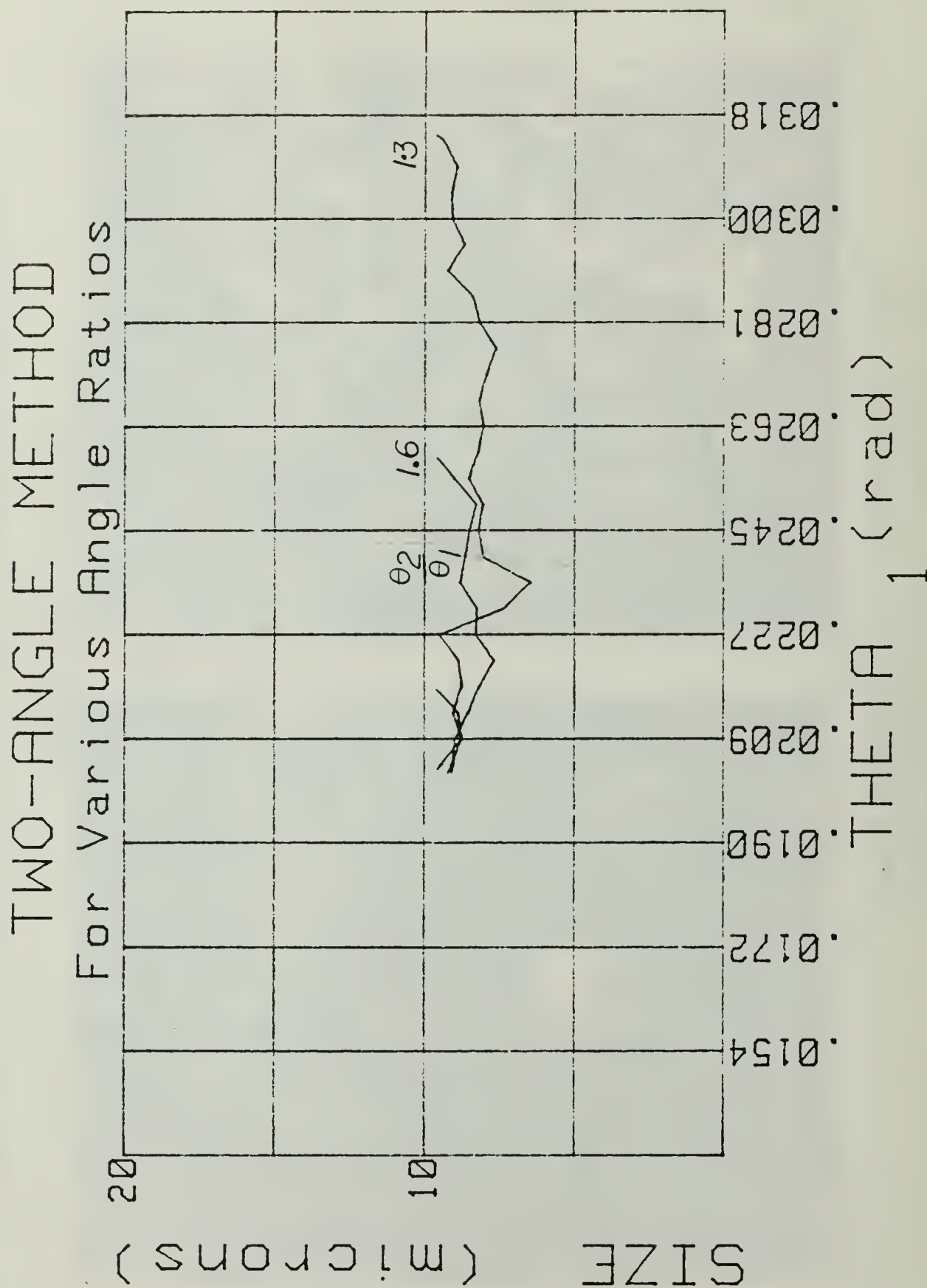


Figure 4.17 Two-Angle Method, 2% Aluminum Propellant, Exhaust



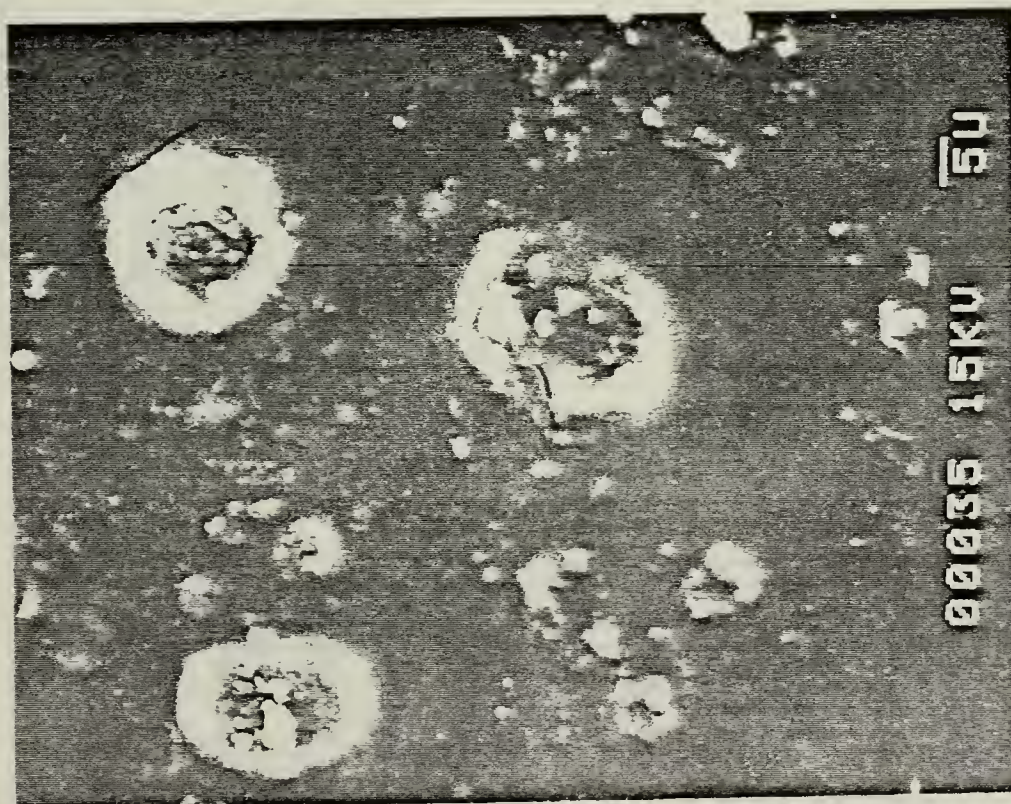
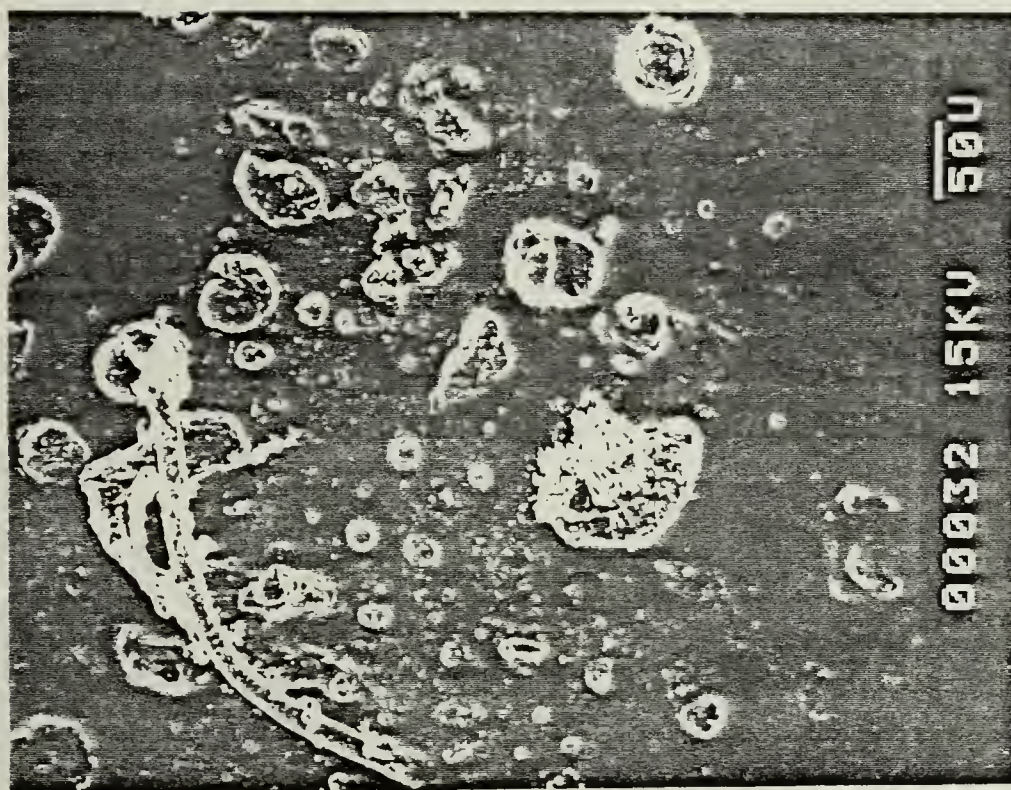


Figure 4.18 SEM Evaluation, 2% Aluminum Propellant, Exhaust

# FILTERED DATA VOLTAGE vs. DIODE

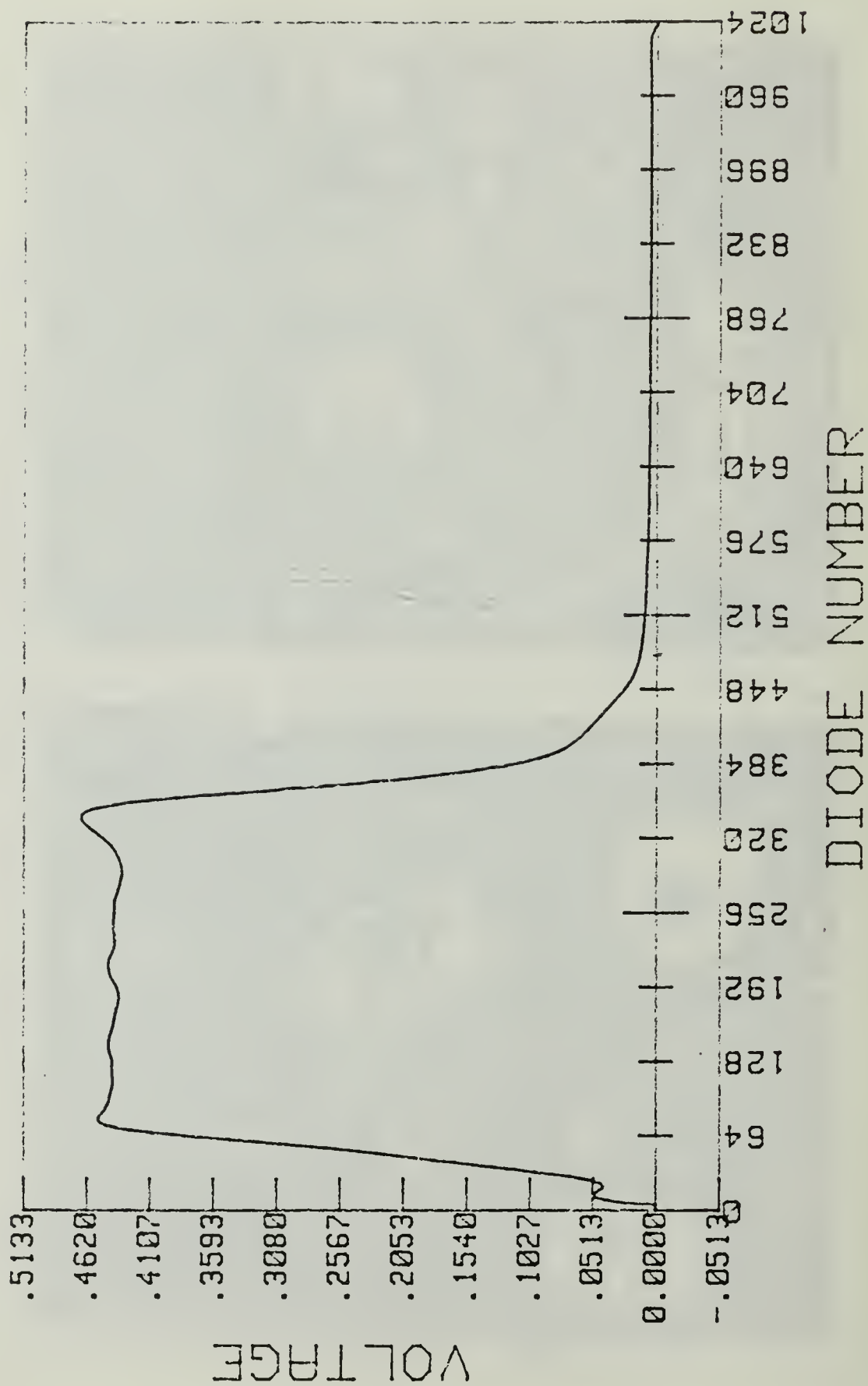


Figure 4.19 Voltage vs Diode, 0% Aluminum, Motor Cavity



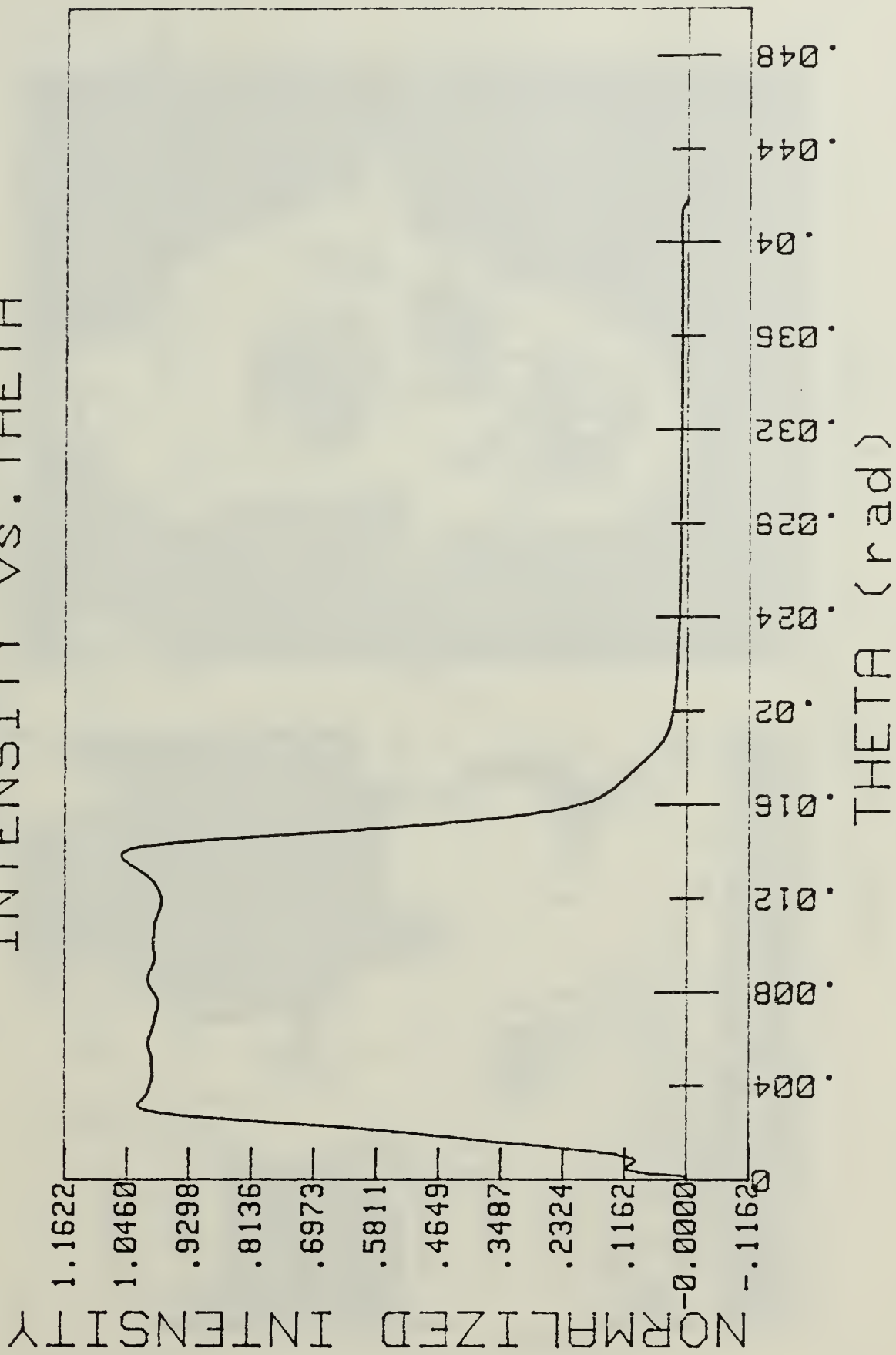


Figure 4.20  $I(\theta)$  vs Theta ( $\theta$ ), 0% Aluminum, Motor Cavity

# FILTERED DATA VOLTAGE vs. DIODE

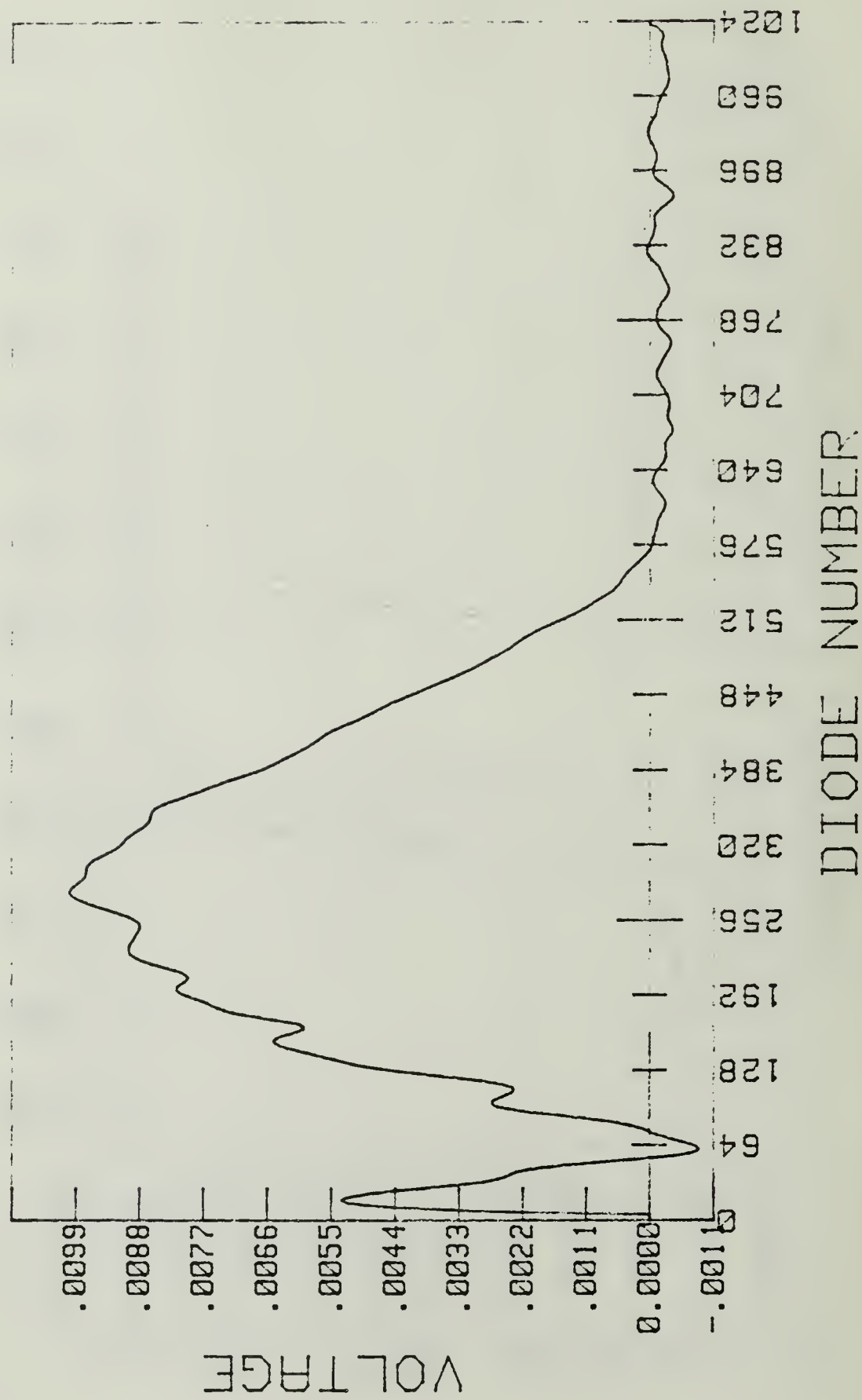


Figure 4.21 Voltage vs Diode, 4.8% Aluminum, Motor Cavity

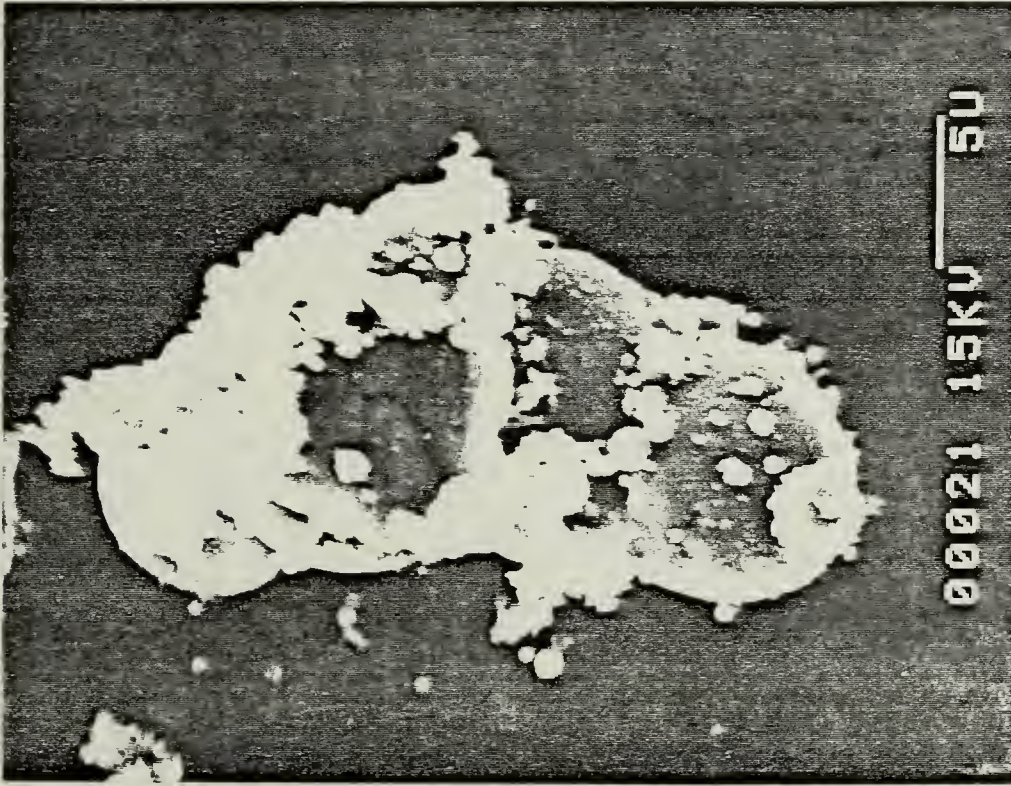
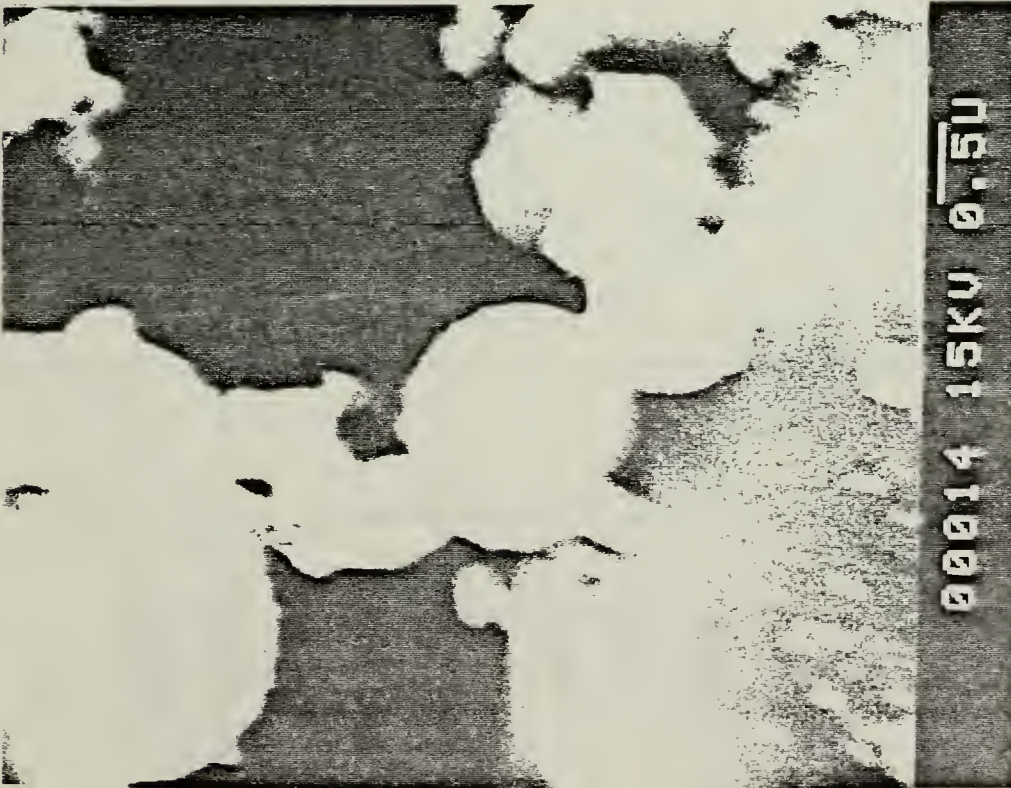


Figure 4.22 SEM Evaluation, 4.8% Aluminum, Motor Cavity



# CURVE FIT RESULTS INTENSITY vs. THETA

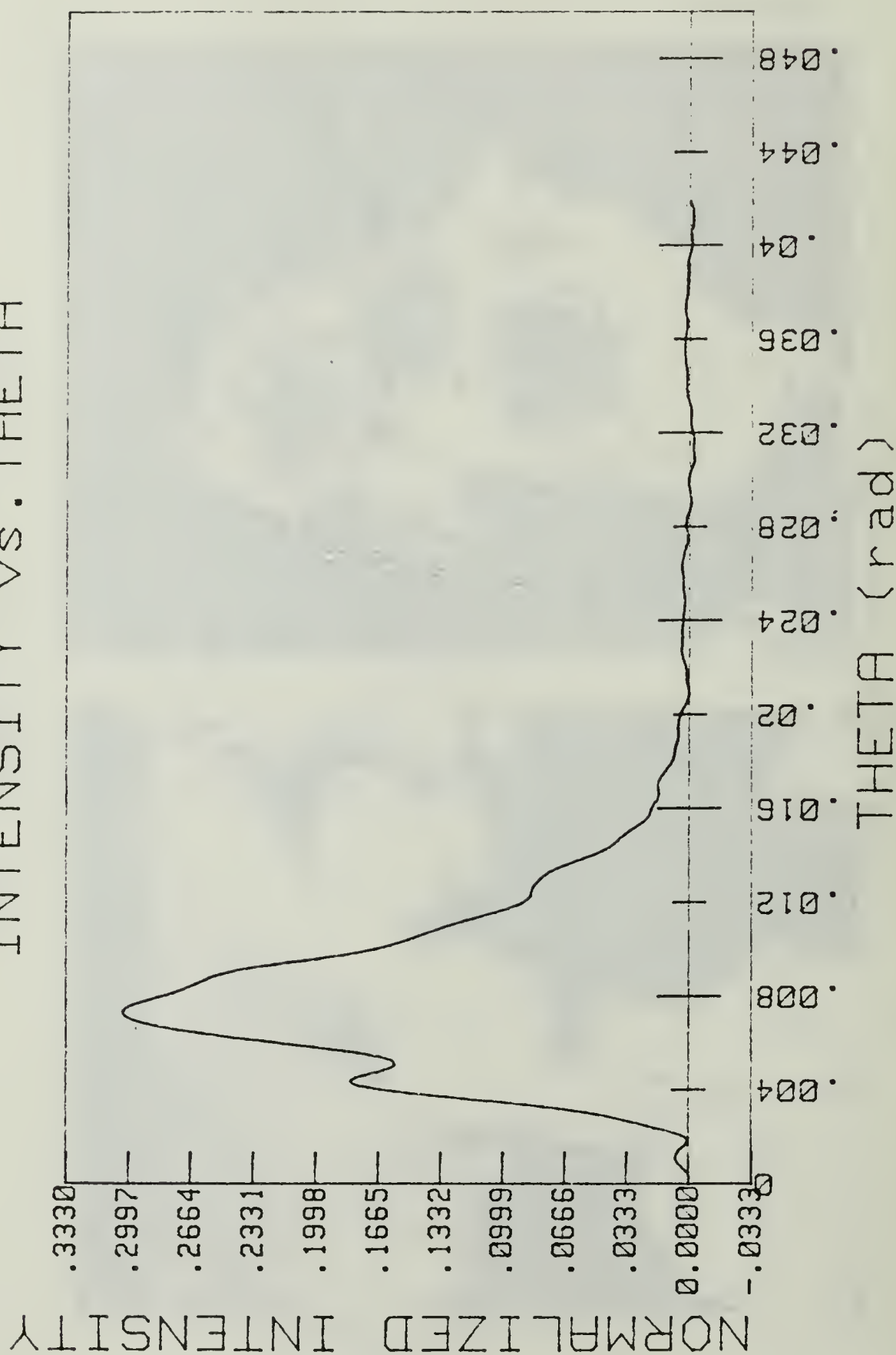


Figure 4.23  $I(\theta)$  vs Theta ( $\theta$ ), 2% Aluminum, Motor, Curve fit

TWO-ANGLE METHOD  
For Various Angle Ratios

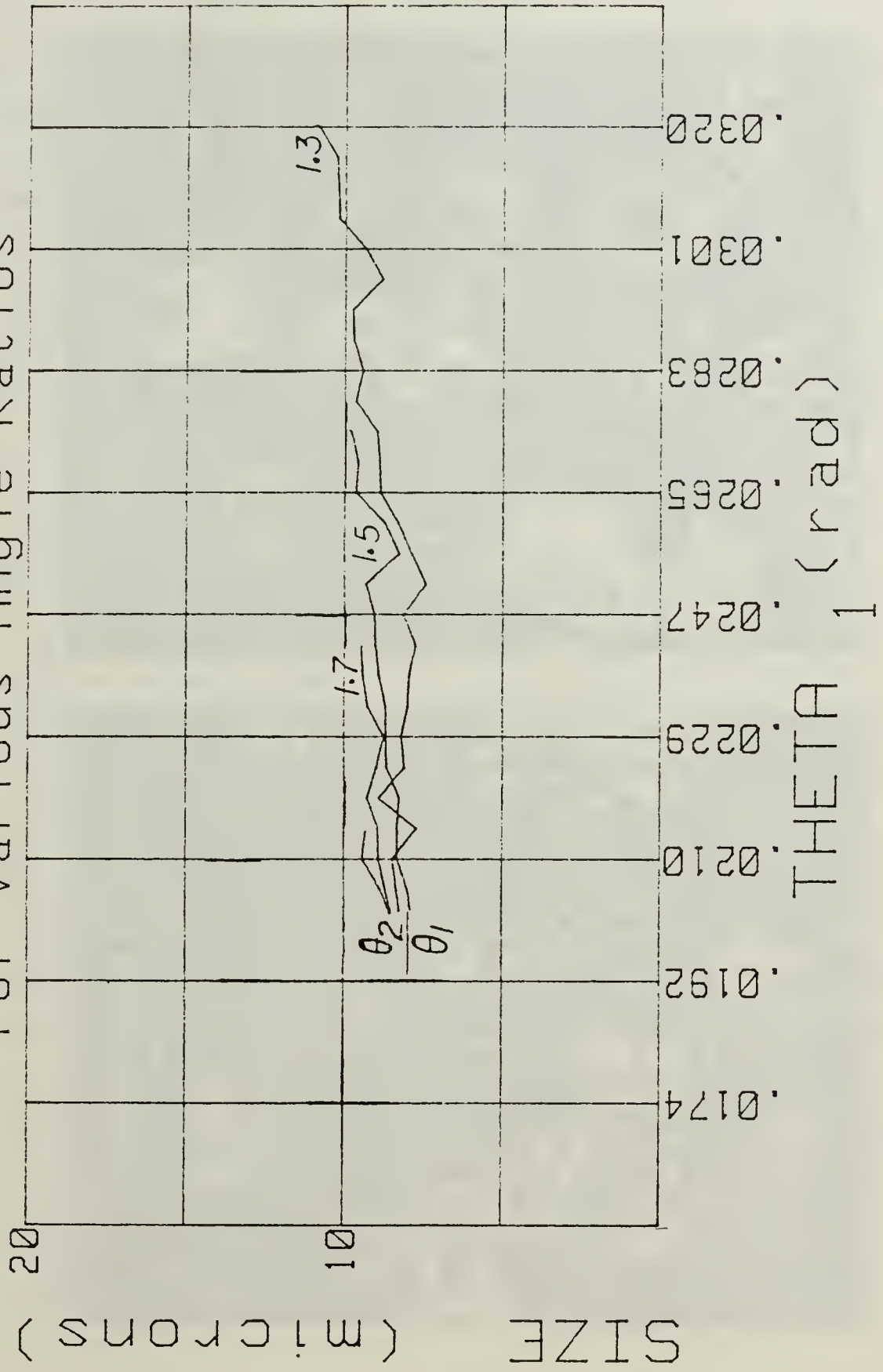


Figure 4.24 Two-Angle Method, 2% Aluminum, Motor Cavity



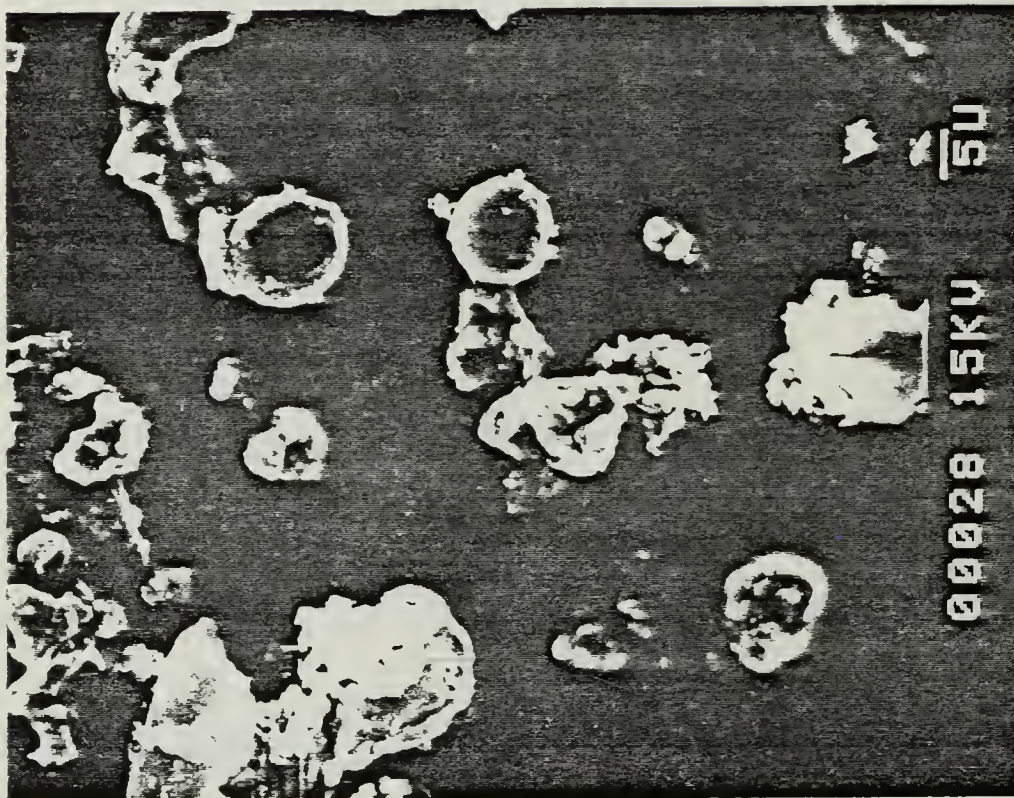
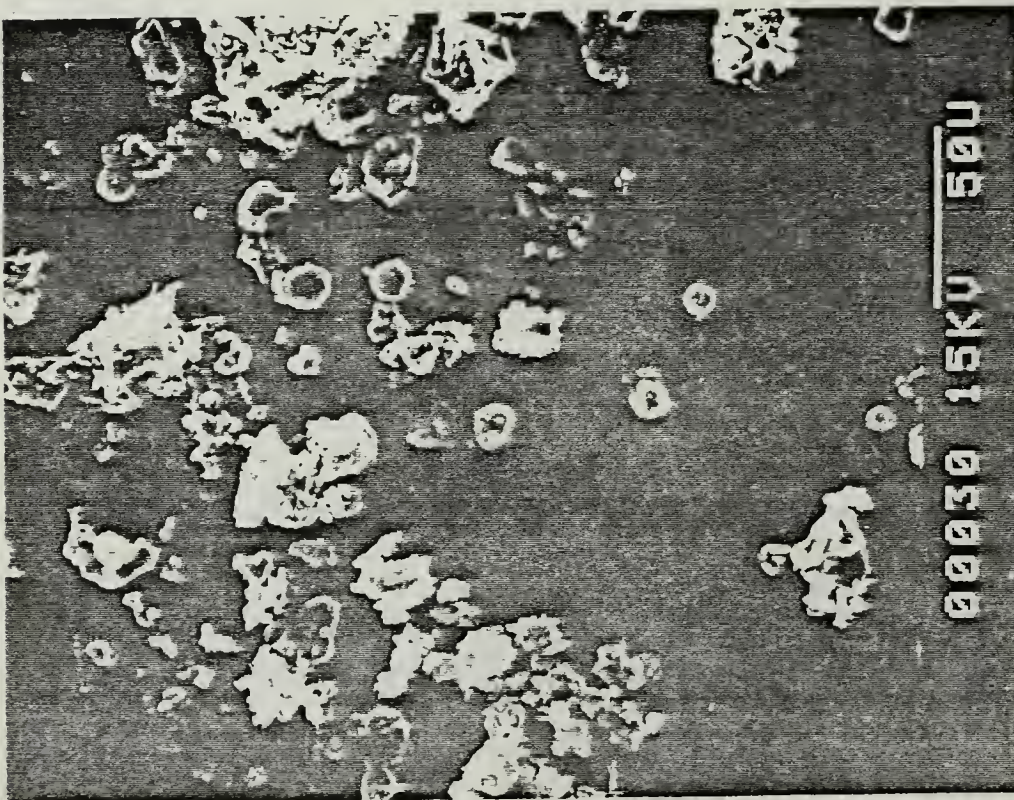


Figure 4.25 SEM Evaluation, 2% Aluminum Propellant, Motor Cavity



## V. CONCLUSIONS AND RECOMMENDATIONS

The results of this investigation have shown that accurate determination of  $D_{32}$  using only measurements of forward scattered light will be difficult. However, with some apparatus modifications the technique appears to be practical, especially if used in conjunction with measurements of transmitted light at multiple wavelengths.

Alignment of the optics was found to be critical when windows must be used in the light beam. Light attenuation is almost always greater than 10%. However, the calibration results indicated that the technique can yield correct particle sizes to transmittances as low as 50%.

$D_{32}$  measurements are biased toward the larger particles in the distribution, as evidenced by the comparison of the collected exhaust particles and the measured particle sizes. The measured exhaust plane particle sizes for both the 4.8% and 2% aluminized propellants and the entrance plane particle size for the 2% aluminized propellant were in reasonable agreement with the particle sizes observed with the SEM.

Several apparatus changes should be made to determine if they would significantly improve the obtainable data. Alignment procedures should ensure that no reflected beams are present from the motor windows. Light transmission measurements should always be made at the same time that the scattering measurements are made to ensure that the scattering data can be properly utilized. Larger beam stops should be used or they could be removed entirely if the diode array were shifted to larger scattering angles (2-5 degree).



## LIST OF REFERENCES

1. Henry, C. and Norman, S. C., "Performance of Solid Propellants Containing Metal Additives", AIAA Journal, Vol 3, No. 2, February, 1965.
2. Beckstead, M. W., Dobbins, R. A. and Brewster, B. S., "Distributed Combustion Effects on Particle Damping", AIAA Journal, Vol 22, No. 3, March, 1984.
3. George, D., "Recent Advances in Solid Rocket Motor Performance Prediction Capability", AIAA Paper AIAA-81-033, 19th Aerospace Science Meeting, Jan 12-15, 1981.
4. Barger, M. E., and George, D. "Metal Particle Size Calculations for Solid Propellant Rocket Motor", 18th JANNAF COMbustion Meeting, Vol I, Pasadena, California, 19 - 23 oktober, 1981.
5. Hermesen, R. W. "Aluminium Oxide Particle Size for Solid Rocket Motor Performance Prediction", AIAA 19th Aerospace Sciences Meeting, St. Louis, Missouri, January 12-15, 1981.
6. Dobbins, R. A., "Remote Size Measurements of Particle Product of Heterogeneous Combustion", Eleventh Symposium (International) on Combustion, page 921, The Combustion Institute, 1967.
7. Dobbins, R. A., and Strand, L. D., "A Comparison of Two Methods of Measuring Particle Size of Al O Produced by a Small Rocket Motor", AIAA Journal, Vol 8, pp. 1544 - 1550, 1970.
8. Cashdollar, K. L., Lee, C. K. and Singer, J. M., "Three Wave Length Light Transmission Technique to Measure Smoke Particle Size and Concentration", Applied Optics, Vol 18, No. 11, pp. 1763-1769, June, 1979.
9. Gumprecht, R. O. and Sliepcevich, C. M., "Scattering of Light by Large Spherical Particles", Journal of Physical Chemistry, v. 57, pp. 90-94, January, 1953.
10. Dobbins, R. A., Crocco, L. and Glassman, I., "Measurement of Mean Particle Size of Sprays from Diffractively Scattered Light", AIAA Journal, v. I, No. 8, pp. 1882-1886, 1963.

11. Roberts, J. H. and Webb, M. J., "Measurements of Droplet Size for Wide Range Particle Distributions", AIAA Journal, v. 2, No. 3. pp. 583, 585, 1964.
12. Mugele, R. A., and Evans, H. D., "Droplet Size Distribution in Sprays", Industrial and Engineering Chemistry, v. 43, pp. 1317 - 1324, 1951.
13. Dobbins, R. A., and Jizmagian, G. S., "Optical Scattering Cross Sections for Polydispersions of Dielectric Spheres", Journal of the Optical Society of America, v. 56, No. 10, pp. 1345, 1350, 1966.
14. Dobbins, R. A., and Jizmagian, G. S., "Partical Measurements Base on Use of Mean Scattering Cross Sections", Journal of the Optical Society of America, v. 56, No. 10, pp. 1351 - 1354, 1966.
15. Hodgkinson, J. R., "Particle Sizing by Means of the Forward Scattering Lobe", Applied Optics, v. 5, No. 5, pp. 839, 844, 1966.
16. Powell, E. A., Cassanova, R. A., Bankston, C. P. and Zinn, B. I., "Combustion Generated Smoke Diagnostics by Means of Optical Measurement Techniques", AIAA 14th Aerospace Sciences Meeting, AIAA Paper No. 76-67, January, 1976.
17. Buchele, D. R., "Particle Sizing by Measurement of Forward Scattered Light at Two Angles", NASA Technical Paper 2156, May, 1983.
18. Van de Hulst, H. C., Light-Scattering by Small Particles, John Wiley and Sons, Inc., New York, 1957.
19. Karagounis, S. G., et al, "An Investigation of Experimental Techniques for Obtaining Particulate Behaviour in Metalized Solid Propellant Combustion", Air Force Rocket Propulsion Laboratory Report, AFRL-TR-82-051, July, 1982.
20. Cramer, R.G., et al, "An Investigation of Experimental Techniques for Obtaining Behavior in Metalized Solid Propellant Combustion", Air Force Rocket Propulsion Laboratory Report, AFRPL-TR-84-014, July, 1982.
21. Harris, R. K., An Apparatus for Sizing Particulate Matter in Solid Rocket Motors, M.S. Thesis, Naval Postgraduate School, Monterey, California, 1983.

# INITIAL DISTRIBUTION LIST

	No.	Copies
1. Defense Technical Information Center Cameron Station Alexandria, Virginia 22314		2
2. Library, Code 0142 Naval Postgraduate School Monterey, California 93943		2
3. Department Chairman, Code 67 Department of Aeronautics Naval Postgraduate School Monterey, California 93943		1
4. Professor D. W. Netzer, Code 67Nt Department of Aeronautics Naval Postgraduate School Monterey, California 93943		3
5. Komandan Jendral Komatau Lanuma Husein Sastranegara Bandung 40174, Indonesia		3
6. Major Abubakar K Jalan Let. Udara Subagio 20 Bandung 40174, Indonesia		5





8  
1 3 5 3 7 5





211933

Thesis

K38942

c.1

Kertadidjaja

Particle sizing in  
a solid rocket motor  
using the measurement  
of scattered light.

211933

Thesis

K38942

c.1

Kertadidjaja

Particle sizing in  
a solid rocket motor  
using the measurement  
of scattered light.



thesK38942

Particle sizing in a solid rocket motor



3 2768 002 12138 6

DUDLEY KNOX LIBRARY